A 2000 year record of marine climate variability from Arnarfjörður, NW Iceland

Ingibjörg Rósa Jónsdóttir

Faculty of Earth Sciences
University of Iceland
2015

A 2000 year record of marine climate variability from Arnarfjörður, NW Iceland

Ingibjörg Rósa Jónsdóttir

60 ECTS thesis submitted in partial fulfilment of a
Magister Scientiarum degree in Geology

Advisors
Áslaug Geirsdóttir
Sædís Ólafsdóttir

Examiner
Katrine Husum

Faculty of Earth Science
School of Engineering and Natural Sciences
University of Iceland
Reykjavík, October 2015

A 2000 year record of marine climate variability from Arnarfjörður, NW Iceland
Climate variability in Arnarfjörður the past 2000 yr
60 ETCS thesis submitted in partial fulfilment of a *Magister Scientiarum* degree in geology

Faculty of Earth Sciences
School of Engineering and Natural Sciences
University of Iceland
Askja, Sturlugata 7
101 Reykjavík
Iceland

Telephone: 525 4600

Bibliographic information:
Ingibjörg Rósa Jónsdóttir, 2015, *A 2000 year record of marine climate variability from Arnarfjörður, NW Iceland*, Master's thesis, Faculty of Earth Sciences, University of Iceland, pp. 58.

Printing: Háskólaprent
Reykjavík, Iceland, October 2015

Útdráttur

Arnarfjörður er annar stærsti fjörður Vestfjarða. Setkjarni, sem var tekinn í firðinum árið 2010, var rannsakaður með það markmið að kanna umhverfisbreytingar í firðinum síðustu 2000 árin. Tveir ólíkir sjávarstraumar hafa hvað mest áhrif á Arnarfjörð, annars vegar flytur Irmingerstraumurinn hlýjan og saltan sjó að landinu úr suðri og hins vegar berst kaldur og seltulítill sjór með Austur-Grænlandsstraumnum úr norðri. Skilin milli þessara tveggja straumakerfa kallast pólarfrontur og hafa þau færst til í gegnum jarðsöguna háð styrkleika straumanna.

Setkjarninn úr Arnarfirðinum býður uppá nákvæm gögn með háa tímaupplausn fyrir síðustu 2000 árin, en það tímabil hefur að geyma bæði hlýindi miðalda (*e. MWP*) og kuldatíma Litlu ísaldarinnar (*e. LIA*). Aldursgreiningar á setkjarnanum benda til að það vanti u.þ.b. síðustu 150 árin í kjarnann eða frá því að Litla ísöldin náði hámarki. Í þessari rannsókn var notast við röntgenmyndir til að greina ísrekið efni, mælingar á segulviðtaki og eðlisþéttleika setsins til þess að rekja uppruna efnis og kolefnismælingar og götungagreiningar til þess að meta lífræna virkni og breytileika í umhverfisþáttum á tímabilinu. Megin áhersla verkefnisins var að greina samsetningu götungafánunnar til að meta og endurskapa hitastig sjávarstraumanna, hafísaðstæður og aðrar umhverfisbreytingar í firðinum.

Breytingar á götungafánunni í Arnarfirði skiptir kjarnanum upp í þrjú tímabil. Það elsta nær frá u.þ.b. 350-800 AD, næsta tímabilið er frá 800-1200 AD og það yngsta frá 1200-1850 AD. Tölfræðilegri úrvinnslu (*e. transfer function method*) var beytt á gögnin til að áætla botnhitastig í firðinum fyrir tímabilið. Aðferðin felst í því að nýta módel sem byggir á nútímasamsetningu á götungafánu og tilsvarandi kjöraðstæðum hennar (hitastig og selta) víðs vegar frá N-Atlanthafssvæðinu. Með því að setja niðurstöður götungagreiningunnar úr setkjarnanum í módelið má reikna út áætlaðan botnhita sjávar síðustu 2000 ára. Niðurstöður benda til að talsverðar sveiflur hafa orðið á hitastigi í firðinum. Fyrsta tímabilið einkennist af frekar stöðugu en kólnandi umhverfi. Miðhluti kjarnans (800-1200 AD) sýnir hlýrri aðstæður, með hæsta áætlaða botnhitann í kringum 1100 AD (4.53 ± 0.646°C), en það er svipaður hiti og er í Arnarfirði í dag. Um 1200 AD fara aðstæður í firðinum að breytast með auknum áhrifum af kaldari sjávarstraumum.

Þessar niðurstöður á gögnum úr Arnarfirði falla vel saman við svipaðar rannsóknir á nærliggjandi svæði, þar sem Litla ísöldin (ca. 1250-1900 AD) einkenndist af mjög óstöðugu ástandi og köldum botnstraumum.

Abstract

A high-resolution sedimentary record from the subarctic Arnarfjörður in northwestern Iceland is being studied, with the ultimate goal to reconstruct the marine climate and the environmental history of Arnarfjörður for the past 2000 years. The fjord provides a regional oceanographic climatic signal reflecting changes in the Irminger Current, a branch of the warm and saline North Atlantic Current and the fresher East Greenland Current from the north, and changes in sea ice cover in the region.

The sediment core spans approximately 2000 years and thus offers a high resolution record for that time interval, which includes both the Medieval Warm Period (MWP) and the early to middle part of the Little Ice Age (LIA). We estimate approximately 150 years missing from the top of the section. The marine climate reconstruction is based on multi-proxy study including; x-radiographs which are used to identify ice rafted debris (IRD), magnetic susceptibility, density, total carbon, x-ray diffraction (XRD) and foraminiferal research. The main emphasis was though on utilizing the benthic foraminifera to describe the oceanographic and environmental changes in the Arnarfjörður region.

This first of the kind study from Arnarfjörður has multidecadal time resolution and demonstrates significant variability in the benthic foraminiferal fauna dominated by *Cibicides lobatulus*, *Cassidulina reniforme* and *Elphidium excavatum*. By applying statistical transfer function methods on the down-core faunal composition estimates on the bottom water temperatures (BWT_{TF}) and salinities (BWS_{TF}) was obtained. For the past 2000 years the estimated BWT's in Arnarfjörður fluctuates from ca. 1.5 ± 1.09°C to 4.53 ± 0.646°C, a variability of ~3° C.

The data from Arnarfjörður is in harmony with previously reported LIA characteristics from the region, which has been described as a period of high amplitude fluctuations, with non-stable conditions and cold bottom waters.

Table of Content

Figures

Tables

Acknowledgements

First and formost I would like to thank my advisors, Áslaug Geirsdóttir and Sædís Ólafsdóttir for their guidance and support throughout this project.

Next, my appreciation goes to people who helped me on the completion of this project.

Ingibjörg Jónsdóttir for assisting me with the multibeam data and everything related to sea ice.

John Andrews at the University of Colorado for the XRD-analysis as well as providing papers and advice.

David Harning for chemical analysis of the crypto-tephra found in the core and Þorvaldur Þórðarson for helping me with the interpreation of the tephra results.

Halldóra Björk Bergþórsdóttir for all of the help, specially with the carbon coulometer.

Sigrún Sif Sigurðardóttir for helping me with the maps in GIS.

.

1 Introduction

The North Atlantic region is sensitive to natural climate variabilities, which are driven by oceanic and atmospheric circulation. Huge amount of heat is transported to the North Atlantic via the North Atlantic Drift (NAD) (Berner et al., 2011), which explains mild climate at high latitudes. Proxy-based reconstructions show a general decrease in Northern Hemisphere (NH) summer temperatures over the past 5 to 4 ka, reflecting the gradual decline in summer insolation (e.g. Alley et al., 1999; Wanner et al., 2011, Geirsdóttir et al., 2013). In recent years, an increasing number of high-resolution Holocene studies have been obtained in the North Atlantic, with the focus on the last millennium or two (Butler, et al, 2013; Eiríksson et al., 2006; Geirsdóttir et.al. 2009; Hald et al., 2011; Jennings & Weiner, 1996; Knudsen et al, 2012; Massé et al, 2008; Sicre et al, 2008, 2013). Most of these studies show two intervals of contrasting climate. The Medieval Warm Period (MWP) is the earlier of these two intervals, occurring approximately from the ninth to the thirteenth century AD. The second climate interval is frequently referred to as the Little Ice Age (LIA) and is considered the most extreme cold summer anomalies over the past 8 ka years (Miller et al. 2012). These decadal to centennial climate variability cannot be explained with decreasing summer insolation alone, but rather suggest combined factors and feedback effects such as volcanic eruptions (Miller et al., 2012) and total solar irradiance minima (Steinhilber and Beer, 2011). One of the most dominant feature in North Atlantic climate variability is the North Atlantic Oscillation (NAO). The NAO strongly influences the speed and orientation of westerly winds from the Gulf of Mexico to northern Europe and drives long-term variations in patterns of circulation and convection (Hurrell et al., 2003).
To better understand and predict future climate changes it is crucial to obtain high-resolution records of past climatic variations and the controlling factors. Instrumental climate records have only a limited span back in time and thus proxy data must be used to estimate variability in climate beyond this time.

Iceland is the largest landmass in the central North Atlantic Ocean. The oceanographic system around Iceland is dominated by the Irminger Current transporting heat and nutrients from the south and the East Greenland Current bring cold and fresh polar water from the north. These two main water masses are separated by the Polar Front (Valdimarsson & Malmberg, 1999). The position of the front varies over time and shapes the climate of Iceland. The Vestfirðir peninsula, the study region, is in close proximity to the Polar Front and thus ideal for reconstructing marine climate variability.

Fjords along the Vestfirðir peninsula capture both the marine and terrestrial climate signal, and thus provide a direct link between land and sea. One of the most interesting features of fjords is that they typically have a higher sediment accumulation rate than the deeper ocean, because they serve as sediment traps to terrigenous sediments eroded from the fjord drainage basin. Sediment records from the fjord environment therefore produce archives, which contain information about variations in marine, terrestrial and atmospheric settings (Howe et al., 2010) and allow study of air-ocean-land interactions in great detail useful for high-resolution Holocene palaeoclimatic and palaeoceanographic reconstruction.

Foraminifers are single-cell protozoa and are generally divided into two main groups: benthic and planktic (Murray, 1991). In the modern environment each foraminiferal species chooses its own favorable ecologic condition, which makes them useful proxy to reconstruct quantitatively oceanographic changes and variability, since faunal distributions and abundances are related to temperature, salinity and marine productivity (Murray, 1991). In fjords, foraminiferal assemblages predominantly consist of benthic species. Low percentage of planktic species is due to fresh input of runoff water from land as well as stronger surface currents.

In August 2010 the National Authority of Iceland (Orkustofnun) in cooperation with the Norwegian Petroleum Directorate (NPD) and the Icelandic Marine Research Institute (IMR) conducted a marine research cruise covering the Dreki area and the Jan Mayen Ridge. The research vessel, Árni Friðriksson RE 200, carried out the sampling campaign and obtained the core A2010-10-586 (65°25.45; 23°33.67) from Arnarfjörður, NW Iceland.

The goal of this project is to reconstruct the marine climate and the environmental history of Arnarfjörður for the past 2000 years driven by the following research questions:

- What do the proxy records tell about environmental changes in Arnarfjörður over the past 2000 years?
- Are there changes in the faunal assemblage of the benthic foraminiferas and how can they be used to reconstruct the environmental change that may have taken place in Arnarfjörður?
- Can we recognize MWP and LIA in the Arnarfjörður record and if so what is the timing of these events?
- What drives climate and environmental variability in Arnarfjörður?
- Can the fjord core be regarded as a link between the open ocean and land, and thus potentially linking the different components of the climate system.

The reconstruction was based on physical inspection of the sediment core by using x-radiographs to identify ice rafted debris (IRD) and applying x-radiograph diffraction (XRD) to gain mineralogical information. As well as, carrying out magnetic susceptibility (MS), total carbon (TC), and density measurements. However, most of the emphasis was on the benthic foraminiferal faunal study where down-core distributional patterns were used to describe the oceanographic settings and identify environmental changes in the study area. The benthic foraminiferal study also allowed applying statistical transfer function method to get estimated bottom water temperature records for the fjord.

2 Geographical settings

2.1 Modern oceanography

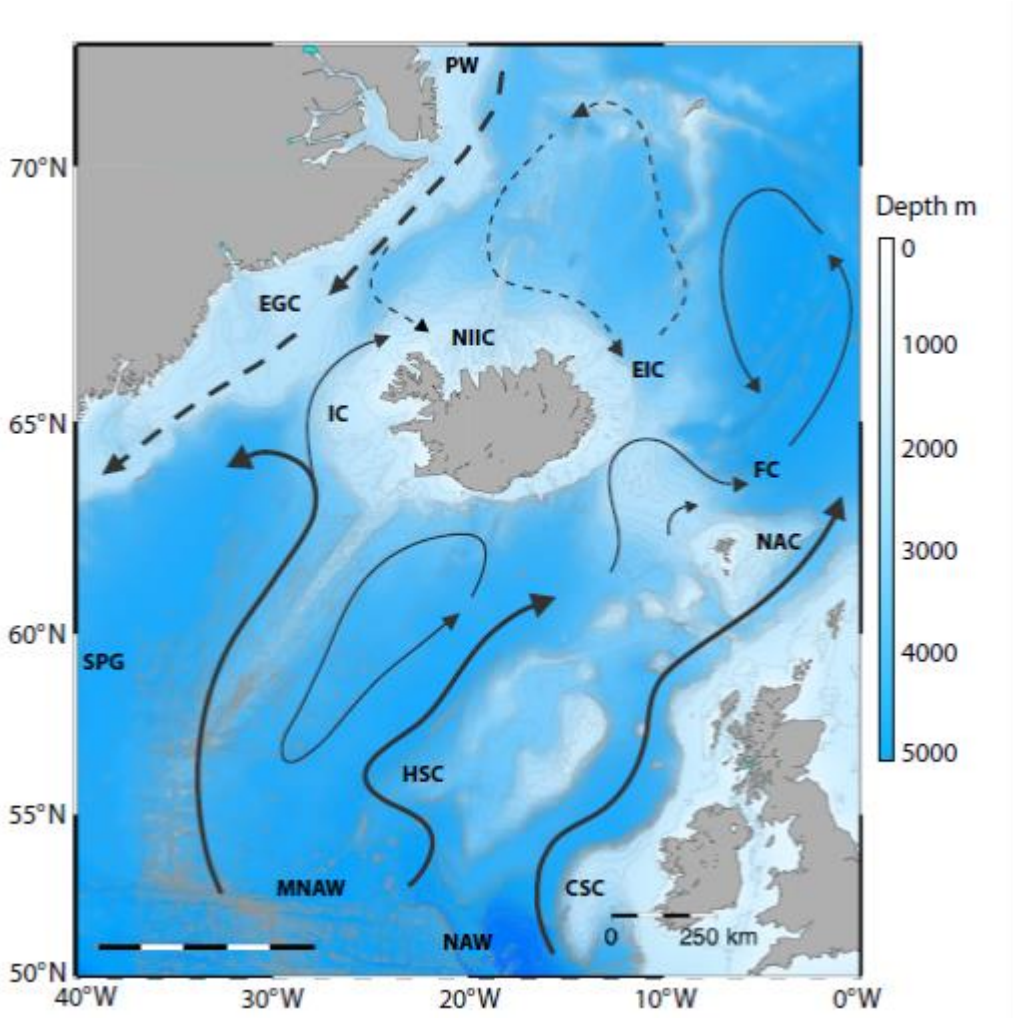

Figure 2-1: Map of the main surface currents around Iceland (PW=Polar water, EGC=East Greenland Current, EIC=East Icelandic Current, NIIC=North Icelandic Irminger Current, IC=Irminger Current, NAC=North Atlantic Current).

Iceland is located slightly south of the Arctic Circle in the North Atlantic Ocean, at the junction of the Mid-Atlantic Ridge and the Greenland-Scotland Ridge, which segments the adjacent Atlantic into four basins. The Reykjanes Ridge is to the south, the Kolbeinsey Ridge to the north, the Denmark Strait to the west and the Iceland-Faroe Ridge to the east (e.g. Logemann et al., 2013). The bottom topography around Iceland plays a major role in determining the flow of ocean currents in Icelandic water (Valdimarsson and Malmberg, 1999).

Iceland is affected mainly by two ocean surface currents, the Irminger Current (IC) coming from the south and the East Greenland Current (EGC) coming from the north (Fig. 2-1). The divide between these two main surface currents locate the Polar front, which has migrated through time (Valdimarsson and Malmberg, 1999). The Irminger Current is a part of the North Atlantic Current (NAC), branching off to the southwest of the Iceland-Faeroe Ridge bringing warm (3-8°C) and salty (~35‰) water towards Iceland (Stefánsson, 1999). The Irminger Current splits in two with one branch forming a cyclonic eddy in the Irminger Sea and the other branch flowing northward, along the W Iceland Shelf, rounding the North-west peninsula of Iceland (Valdimarsson and Malmberg, 1999). The North Iceland Irminger current (NIIC) is a northward flowing branch of the Irminger current. Farther offshore, to the northwest of Iceland the East Greenland current brings cold (≤0°C) and fresh (<34.4‰) Polar water towards the Denmark Strait. Part of this water enters the Iceland Sea, where it is mixed with Atlantic Water and through cooling of this mixture an arctic water mass is created that subsequently flows within the East Icelandic Current along the continental slope north and east of Iceland and then along the northern flank of the Iceland Faroe Ridge. Branching off northwest of Iceland the East Greenland Current flows as the East Icelandic Current (EIC) eastward along the north Iceland shelf (Stefánsson, 1999). Finally, a coastal current runs in a clockwise direction around Iceland (Valdimarsson and Malmberg, 1999).

2.1.1 Hydrography

Since 1950 the Marine Research Institute (MRI) has conducted annual observation of temperature and salinity at a number of fixed positions on the Icelandic shelf. These stations are along sections that are named after places on shore (Fig. 2-2). After 1970 MRI increased measurements along these transects to four times a year; in February, May, August and November (*www.hafro.is*). The bottom water temperature on the shelf of Iceland is normally lowest in February-March and highest in August-September or even as late as November. The MRI also monitors other aspects during these cruises such as measurements on nutrients and phytoplankton primary production.

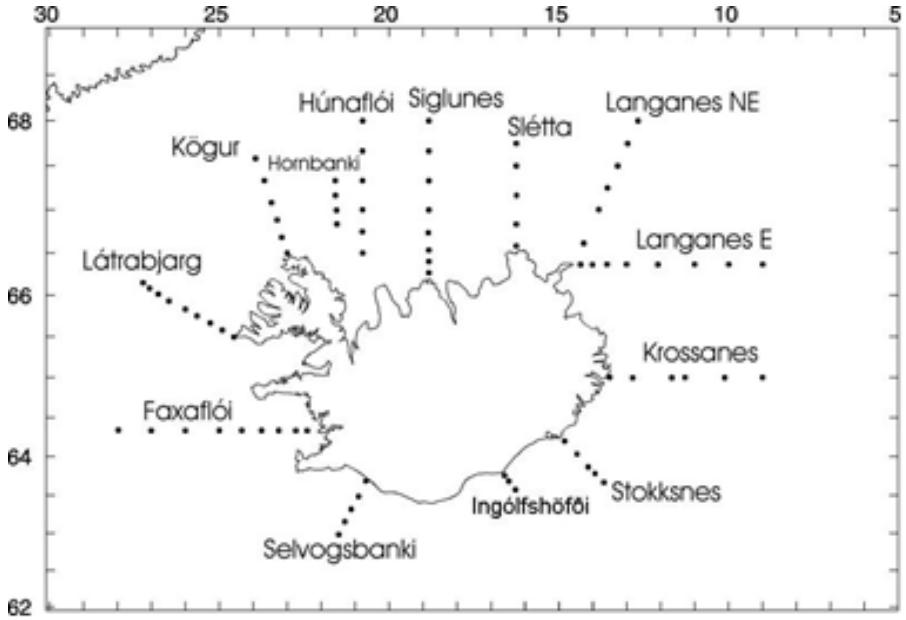

Figure 2-2: Fixed positions on the shelf of Iceland where temperature and salinity measurements are carried out (www.hafro.is)

The annual observation of temperature and salinity on the Icelandic shelf has proven useful in tracing oceanographic or climatic variations, such as The "Great Salinity Anomaly" (GSA) of 1968–1982. The GSA formed during the extreme negative phase of the NAO and under the influence of northerly winds, the polar water and sea ice advanced and lowered the surface salinity of the EIC. The water became effectively stratified and sea ice could form (Steele et al., 2009).

2.1.2 Sea ice and climate

Sea ice occurs primarily in the Polar Regions. Sea ice extent is driven by climate and can affect atmospheric and hydrographic conditions in high latitudes on various timescales (Polyak et al., 2010).

Sea ice can be divided into drift ice and fast ice. Drift ice moves because of wind, surface ocean currents, or other forces. Fast ice (*land-fast ice*) forms at the coastline. After the ice foot breaks up in the spring, remnants often remain buried in beach sediment that can erode the shoreline (Wadhams, 2000). Fast ice is defined by the fact that it does not move with winds or currents. Fast ice can be formed in situ from sea water or by pack ice freezing to the shore, and may extend a few meters or several hundred km from the coast.

Sea ice has a bright surface which reflects 80-90% of the solar radiation falling on it back to space. As a result, areas covered by sea ice do not absorb much solar energy, so temperatures in the Polar Regions remain relatively cool. Open water reflects only about 10%, so the shrinking of the sea ice cover due to climate warming would lead to more radiation being absorbed by the earth resulting in increased amplification of warming (Wadhams, 2000).

Sea ice can reach the coast of Iceland via the East-Greenland Current, which is one of the major sea-ice and freshwater export from the Arctic Ocean (Jennings and Weiner, 1996). The extent of the ice flow varies from year to year. Under normal conditions the main ice edge does not reach the coast of Iceland, whereas in severe ice years, like during the GSA, the ice may extend along the northwest coast of Iceland (Einarsson, 1976).

It is uncommon for sea ice to extend as far south as Arnarfjörður. The most likely situation is when there is a long lasting wind blowing from the west or south-west (Gunnarsdóttir, 2014). An example of that occurred in January 2007 when sea ice reached Arnarfjörður and closed off a small nearby fjord called Dýrafjörður. Sea ice was scarcely reported in Arnarfjörður during the GSA (1968-1969), even though it was commonly found along the coast north and northwest of Iceland.

2.2 Modern climatology

There are several factors, both meterological as well as geographical, that influence the weather and climate in Iceland. One of those factors is the surrounding ocean (maritime climate), which transfer heat from lower latitudes, and causes fairly mild winters and cool summers in Iceland with rather small annual range of temperature (i.e. the difference between the average temperatures of the warmest and coldest month). The history of meterological observation in Iceland goes back to 1749-1750 when instrumental observations were carried out near Reykjavík. The first meterological station with systematic and continuous weather observation was established at Stykkishólmur in 1845

and has been in operation ever since (Einarsson, 1976). Temperature readings from 1901-1990 at the Stykkishólmur station show a mean winter (January – March) temperature of 0.9°C and mean summer (June – August) temperature of 9.3 °C (Einarsson, 1976).

Another factor that also strongly influences the climate in Iceland is the North Atlantic Oscillation (NAO), which is the most important mode of atmospheric variability over the North Atlantic Ocean (Hurrell et al., 2003). The NAO consists of two pressure centers in the North Atlantic, one is an area of low pressure typically located near Iceland and the other an area of high pressure over the subtropical Atlantic (Azores High). The pressure difference is most noticeable during the boreal cold season (November-April) and is associated with changes in the mean wind speed and direction (Hurrell et al., 2003). A fluctuation in the strength of these features significantly alters the alignment of the jet stream, especially over the eastern U.S., and ultimately affects temperature and precipitation distributions in the North Atlantic area. In other words, the NAO measures the strength of the westerly winds blowing across the North Atlantic Ocean in the 40°N - 60°N latitude belt.

To get an overview of changes in the North Atlantic Oscillation over a period of time, Hurrell (1995, 1996) defined an index for the NAO (Fig. 2-3). It is based on the difference of normalized sea level pressure (SLP) readings from two stations, one on Iceland and the other one either in the Azores, Lisbon or Gibraltar. The winter NAO index reflects the variance between daily readings from November through March and the averaged values (Hurrell et al., 2003). In figure 2-3 the NAO index shows low values during the period from the early 1950s to the early 1970s (GSA) and high values for the last 25 yr. The corresponding index varies from year to year, but also exhibits a tendency to remain in one phase for intervals lasting several years.

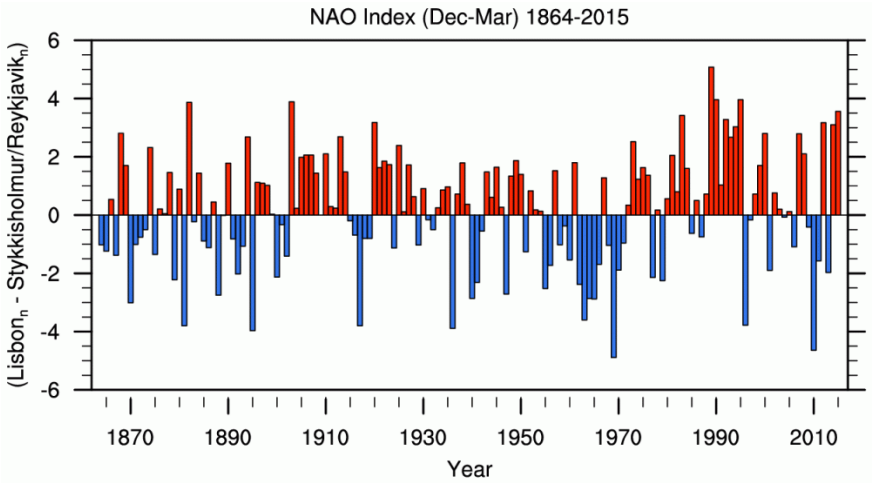

Figure 2-3: The North Atlantic Oscilliation Index (Hurrell, 2015).

Figure 2-4 demonstrates negative and positive phases of the NAO. The negative NAO phase shows a weak subtropical high and weak Iceland low. The NAO has a major influence on storm tracks, with reduced activity in the northeastern part of the North Atlantic when the index is low. During negative NAO the westerly winds are weaker than normal and the pressure difference is smaller resulting in reduced Atlantic Water advection

and cold/dry conditions over NW Europe (Hurrell, 1995). The USA east coast experiences more cold air outbreaks and snowy weather conditions, Greenland, however, will have milder winter temperatures (Hurrell, 1995).

Conversely positive NAO index phase shows a stronger than usual subtropical high pressure center and a deeper than normal Icelandic Low. The increased pressure difference results in stronger winter storms crossing the Atlantic Ocean on a more northerly track. This results in warm and wet winter in North Europe but drier conditions over much of central and southern Europe and wetter than normal conditions over Iceland and Scandinavia. Additionally, the Eastern USA experiences mild and wet winter conditions while the eastern Canadian Arctic is colder than normal (Hurrell, 1995). When the NAO index is high the Greenland Sea experiences less severe winter conditions than normal leading to reduced deep convection activity and the opposite is true when the NAO index is low.

Changes in the NAO phases induce significant changes in ocean surface temperature and heat content, ocean currents and their related heat transport, and sea ice cover in the Arctic and sub-Arctic regions (Hurrell et al., 2003). The NAO alone can account for 31% of the winter surface temperature variance over the northern hemisphere north of 20°N (Hurrel, 1996).

Changes in winter temperature associated with the NAO extends all the way across the Eurasian continent from the Atlantic to the Pacific and is thus an indication that the NAO is not a regional North Atlantic phenomenon but rather a hemispheric mode of variability like the Arctic Oscillation (Thompson and Wallece, 1998).

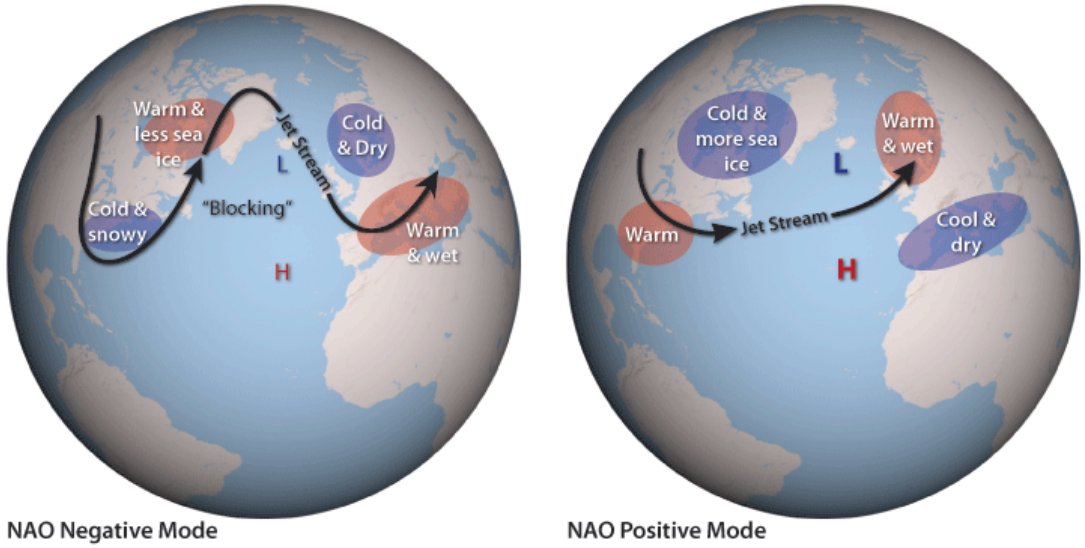

Figure 2-4: NAO negative (left) and NAO positive (right). The variation in pressure patterns influences the strength and location of the jet stream and the path of storms across the North Atlantic (image from: climate.gov, adapted from AIRMAP by Ned Gardiner and David Herring, NOAA).

2.3 Arnarfjörður

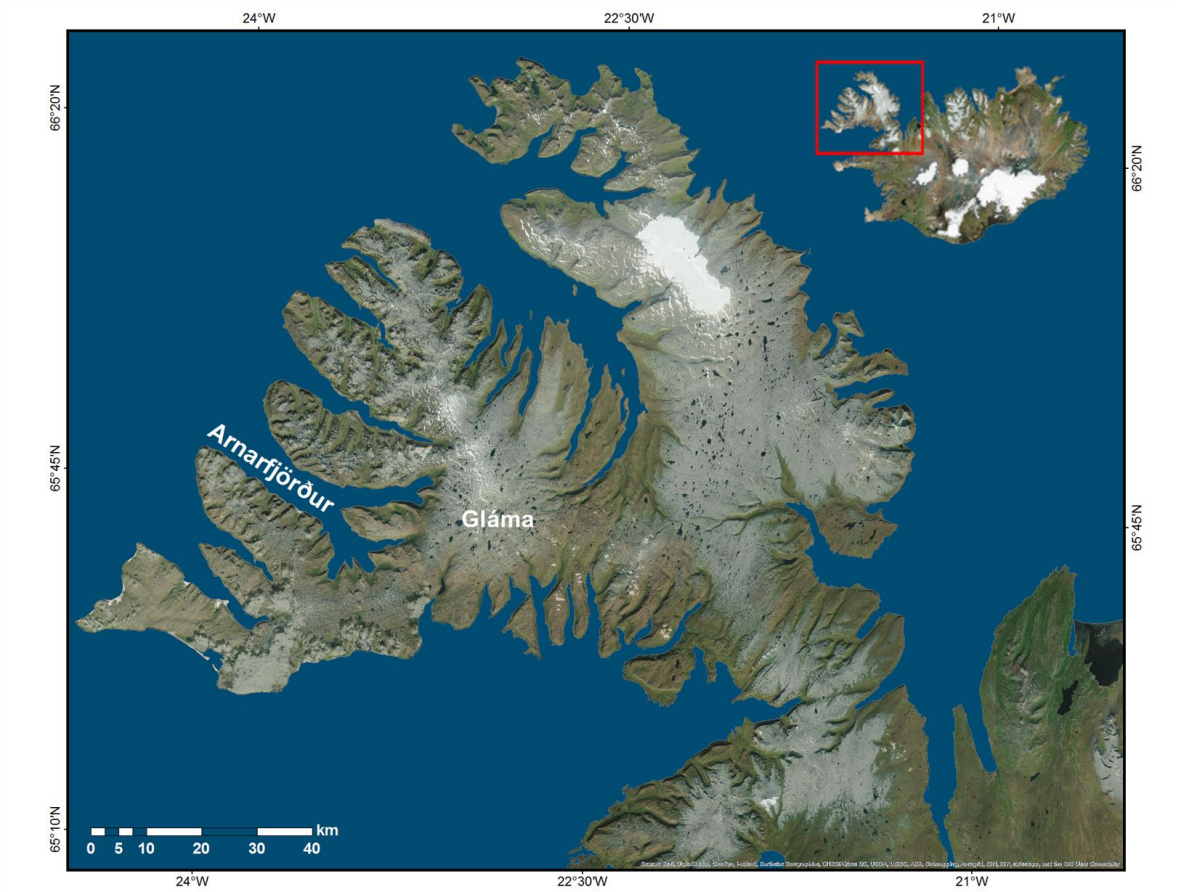

Figure 2-5: Location map showing the study site, Arnarfjörður, and the highland area east of the fjord called Gláma.

The Northwest peninsula of Iceland, Vestfirðir, is mostly composed of Tertiary basalt lava sequences cut by steep-sided fjords (Thors, 1974). The age of these lavas reaches back to about 15 million years, being the oldest known exposed rocks in Iceland (Kristjánsson, 2009). Arnarfjörður is the second largest fjord in Vestfirðir, 30 km long and 5-10 km wide, located between Dýrafjörður in the north and Tálknafjörður in the south (Fig. 2-5). Like other fjords in Iceland it is glacially carved and has a threshold or a sill at the mouth of the fjord. Towards its head it divides into two main tributaries; Borgarfjörður and Suðurfirðir separated by Langanes. A central volcano, which is exposed north of the central part of Arnarfjörður, may be the source of some of the extrusives and dikes that have been seen south of the fjord (Kristjánsson, 2009).

The highest peak in Vestfirðir is called Kaldbakur and rises almost 1000 m above sea level, north of Arnarfjörður. The area east of Arnarfjörður, called Gláma, rises 900 m above sea level. The existence of a glacier on the Gláma plateau has been extensively debated over the time. In the early literature the term Glámajökull (e. Gláma Glacier) was commonly used by Icelanders in the region as well as being shown on geological maps of the area. The highest peak of Gláma is called Sjónfríð (905m) and in 1806 a cairn was built there for geodetic purposes. It is still standing today which speaks against a glacier cover during the last century of the Little Ice Age, but that does not exclude the existence of glacier in the

lower passes between the peaks or as isolated ice masses in cirque basins (Sigurðsson, 2004). Freshwater input to the fjord comes from numerous rivers along the coastline.
The first description of Arnafjörður in the Icelandic historical accounts comes from the time of Hrafna-Flóki's visit around 865 AD, but the accounts suggest that he gave the island the name Iceland after having seen Arnarfjörður covered with sea ice (Landnáma). This is probably the first description of severe sea ice in Iceland's fjords.

2.3.1 *Multibeam measurements*

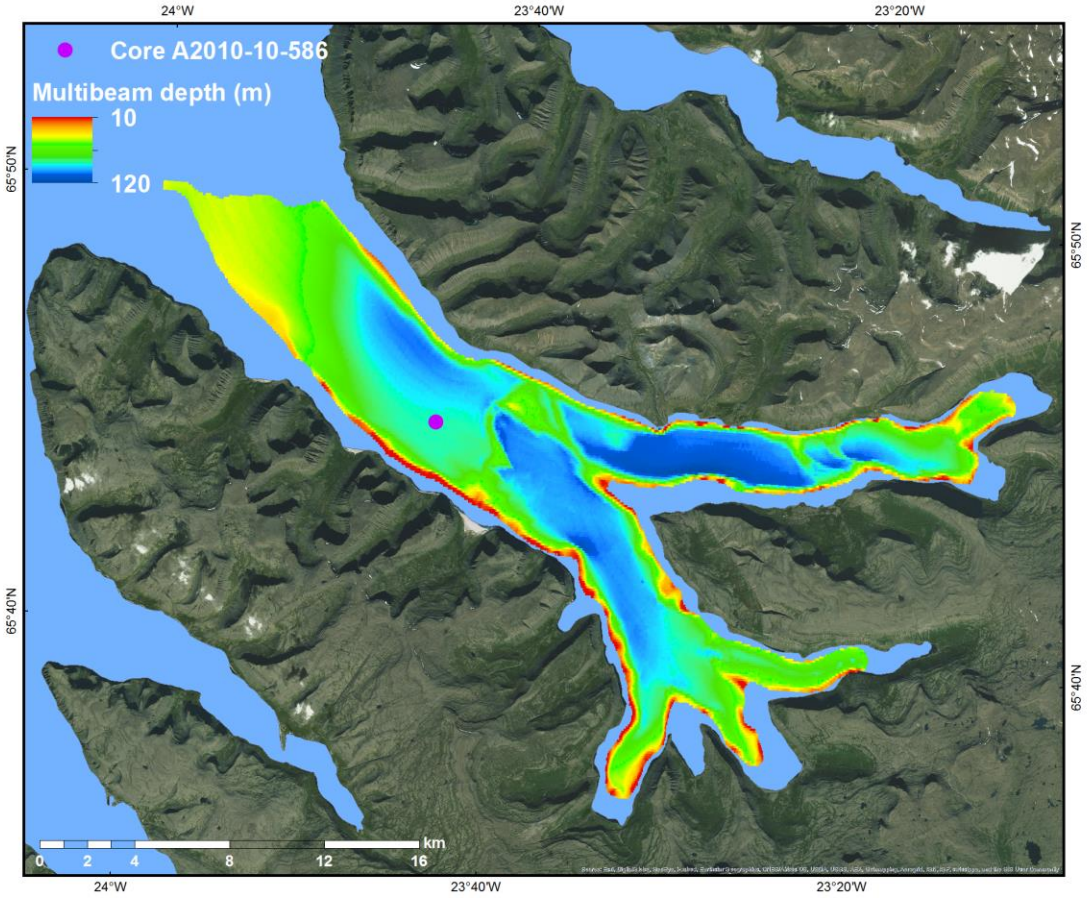

Figure 2-6: Multibeam measurements from Arnarfjörður (www.hafro.is).The location of core A2010-10-586 is shown with a purple dot.

In 2001 and 2002 MRI mapped the seabed of Arnarfjörður. These measurements were part of a bigger project, which started in the year 2000 with the launching of the research vessel Árni Friðriksson. The seabed was mapped with Simrad EM 300 multibeam echosounder with the main goal of obtaining detailed information of the bathymetry and seabed classification (*www.hafro.is*). The measurements show that the fjord is a typical threshold fjord, with the mouth of the fjord much shallower than the head (Fig. 2-6). The average depth of Arnarfjörður is about 90-100 m. There are multiple morainal ridges identified within the fjord, reflecting the advances/retreat of the Icelandic ice sheet during the last deglaciation in the area. The ridges indicate cross-cutting relationship between outlet glaciers from Borgarfjörður and Suðurfirðir as well as a couple of morainal ridges towards the head of Borgarfjörður (Fig. 2-6).

2.3.2 Hydrography of Arnarfjörður

Several transects of annual observation done by MRI circle Iceland (coast towards the shelf edge). The closest transects to the core site are the Látrabjarg and Kögur transects (Fig. 2-2). Based on these transects temperature and salinity profiles are constructed, the Látrabjarg profile lies just south of Arnarfjörður and is influenced more by the Irminger Current compared to the Kögur profile, to the north. The location of the Kögur profile is fairly close to the position of today's polar front, the boundary between the cold East Greenland Current and the warmer Irminger Current. In both profiles, for August 2010, similar trends in temperature (7°C) and salinity at ca. 100 m depth is observed.

In June 2005 and October 2006 two temperature and salinity profiles were made across Arnarfjörður, one of them very close to the core location (Fig. 2-7). The temperature profile shows bottom water in October at ca. 5.5°C and around 7.5°C closer to the surface. The salinity in the fjord is around 34.5‰ at the bottom but decreases upwards to about 34.4‰. The profile for June shows summer stratification in the fjord system, with a 40 m thick surface layer of 7 to 8°C and salinity of 34.35 to 34.45 ‰ and bottom waters of 3°C and salinity of 34.5‰.

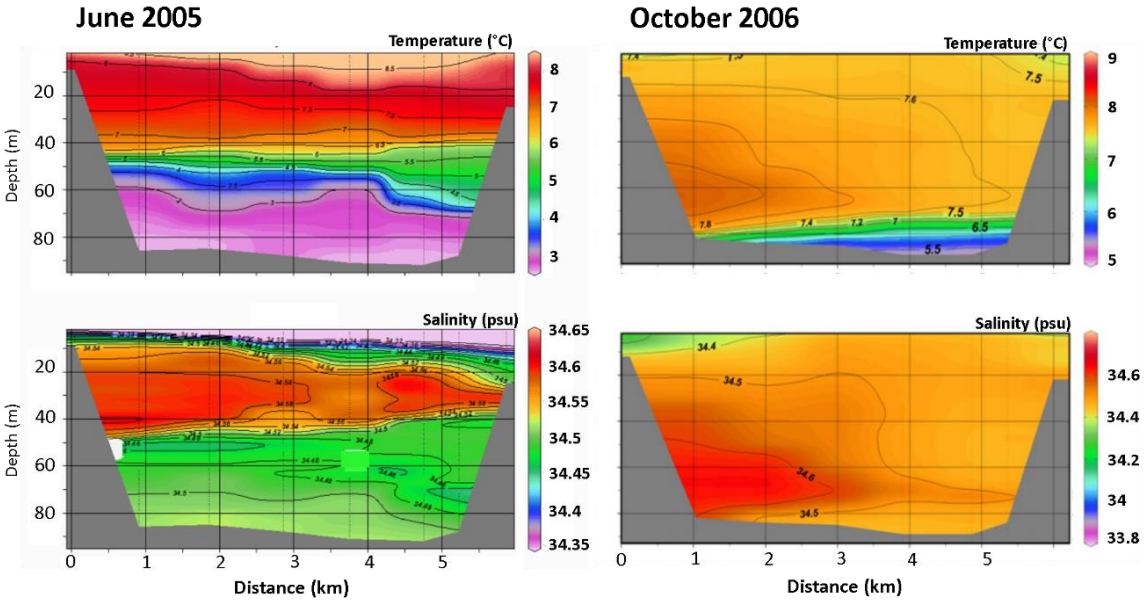

Figure 2-7: Temperature and salinity profiles in Arnarfjörður, taken in June 2005 and October 2006

This stratification of fresher surface water is typical in fjords, which are generally classified as highly stratified estuaries. The flow pattern of water, in a fjord, is known as estuarine circulation, the fresher water will have an outflow along the surface while the more saline water will flow into the fjord beneath the out-flowing layer (Inall and Gillibrand, 2010).

The stratification is caused by the density differences in the early spring costal current and the existing cold fjord water. In September or October the surface water temperatures cool sufficiently to become denser than the underlying water masses and sinks to the bottom and the water column in the fjord mixes. Both oxygenated and nutrient-rich waters are then

brought to the ocean floor leading to increased productivity. Measurements from the fjord also show that the water temperature is lowest in February and March. The temperature increases in April but the water column is still mixed. In June the surface temperature is around 5.5 °C and in July the fjord becomes stratified and does not mix until October (Gunnarsdóttir, 2014). The average current velocity in Arnarfjörður was also measured in 2005 and 2006. The inflowing currents were 3.7 cm/s and the outflow 3.2 cm/s. Inflow to the fjord occurs on the south side of the fjord but the outflow on the north side.

The two most dominant wind directions west of Arnarfjörður are from the SW (50% of the time) and from the NA (30% of the time). Winds blowing directly into the fjord, from the NW, are rare (Gunnarsdóttir, 2014). The average wave height entering Arnarfjörður is thus rather low, but under certain circumstances, especially when the wind direction is from the NW, the waves can reach about 2 to 3 m in height. Fast ice is fairly common in Icelandic fjords such as Arnarfjörður where sufficient input of freshwater exists. The freshwater floats on top due to density difference and when it is cold enough it freezes. When the fast ice breaks up it drifts out the fjord with the currents and eventually melts.

3 Materials and method

Core A2010-10-586 (65°25.45; 23°33.67) was obtained in August 2010, during a research cruise on the research vessel Árni Friðriksson RE 200, a collaborative project of the National Authority of Iceland (Orkustofnun), the Norwegian Petroleum Directorate (NPD) and the MRI. The coring equipment consisted of Benthos Model 2175 piston corer, which has a 6.7 cm inner core liner diameter, with capacity to obtain samples up to 6 m long. The sediment core is 520 cm long, collected from 98 m depth from the middle part of the fjord (Fig. 2-6). The core was packed and brought to the Institute of Earth Sciences, University of Iceland for initial processing, description and subsampling.

3.1 Physical analysis

The reconstruction of the paleoenvironmental conditions is based on physical inspection off the sediment core, x-radiographs, which are used to detect sedimentary structures, molluscs and ice rafted debris (IRD), together with physical proxies such as magnetic susceptibility and density records. The analyses also include total carbon and x-ray diffraction measurements.

3.1.1 Magnetic susceptibility and density

Physical properties, such as density and magnetic susceptibility, normally indicate the proportion of minerogenic to total biogenic material. It can therefore be used to interpret the proportion of terrestrial versus marine material to the core site, and in some cases the presence of tephra layers within a core. Variation in the magnetic susceptibility is a function of mineralogy, grain size and amount of magnetic material. Due to close proximity to land it is highly likely that the increased minerogenic flux into the fjord would reflect increased runoff from land and thus indicating higher landscape instability reflecting colder climate or increased precipitation. The density (ρ) of a material is a measure of how tightly the matter within it is packed together. The Gamma density data can provide a precise and high resolution record of bulk density, and indicate the lithology and porosity changes.

Whole core magnetic susceptibility and density was measured every 2 cm using a Geotek Multi-Sensor Core Logger (MSCL) at the Institute of Earth Sciences, University of Iceland. The core segments were then split and the MS and density of the archive half was measured at higher resolution, or every 0.5 cm, with the Bartington point sensor (MS2E) and the gamma-ray attenuation porosity evaluator (GRAPE) logging system.

3.1.2 X-ray radiographs

X-ray radiographs are important tool for visualizing and recording 3-D structures within the sediment core that may be unrecognizable to the naked eye. They aid in identifying laminae or other sedimentary structures and to characterize grain size trends within a given sequence.

The archive half of the core was radiographed in Orkuhúsið on Tosrad radiographic system. The radiographs were mainly used for identifying shells in the core for the radiocarbon dating and detection of IRD by counting the number of clasts > 2mm (Grobe, 1987). The distribution of IRD is an important parameter in glaciomarine sediments as more IRD generally indicates more sea ice/icebergs interpreted as reflecting colder times.

3.1.3 X-ray diffraction (XRD)

The XRD measurements were carried out at INSTAAR, University of Colorado, Boulder on core samples every 10 cm.

X-ray diffraction can be used to determine the composition of the sediment and to detect tephra that are not visible by eye or on x-radiographs (Andrews et al., 2006). As carbonate bedrock is not found in Iceland's geology, the carbonate content of the sediment is an integrated measure of marine productivity, reflecting changes in carbonate-secreting marine organisms (Andrews et al., 2001). Therefore the weight% of calcite is a measure of surface water stratification and nutrient supply (Andrews and Jennings, 2014). The weight% of quartz is, however, a measure of drift ice transport (Andrews and Jennings, 2014) because Icelandic sediment is rich in basaltic grains and low in quartz or other lithics (Andrews and Principato, 2002).

3.2 Biogenic analyses

The total carbon in sediments represents all the carbon in the sample, both inorganic (TIC) and organic (TOC). The TOC includes traces of vegetation and organisms and is often a measure of marine productivity. The TIC includes the carbonate, bicarbonate, and dissolved carbon dioxide (CO_2). One of the most common carbonates is calcite ($CaCO_3$), which is the main component of limestone as well as mollusc shells and coral skeletons.

Samples for total carbon analysis were run on a CM5200 Automated Combustion Furnace device (combusted to 950°C) and then measured with a carbon Analyser by UIC (CM5014) CO2 Coulometer, at the University of Iceland, with a detection limit of 0.01 wt.%. Approximately 20 mg bulk material was measured every 5-8 cm or total of 75 samples. Usually the TOC of the sample is calculated by subtracting the TIC from the TC. However, due to a failure in the TIC system of the coulometer it was not possible to measure the TIC and therefore only the TC is presented here.

3.3 Foraminifera analyses

Samples for the foraminifera analysis were taken at ca. every 10 cm. They were first freeze dried, then soaked in sodium metaphosphate ($Na(PO_3)_{13}$) solution to prevent clay flakes sticking together. After this procedure the samples were wet sieved with 63, 106 and 1000 µm sieves and then dried. Foraminifera were picked from the 106 µm size sieve. It is often recommended in the literature to count and identify 400 foraminifera individuals from each sample. Statistical test made by Ólafsdóttir (2004) indicated no extreme difference between counting 200 or 400 individuals. It was concluded that counting 200 individuals gives accurate results and therefore, in this study, < 200 benthic foraminifera specimens were picked and identified to species level from each sample. In total 66 samples were counted.

3.4 Chronology – radiocarbon dating

Radiocarbon dating was performed on four marine bivalve shell (depth: 36cm, 164cm, 305cm and 514cm) samples with an accelerator mass spectrometer at INSTAAR, Laboratory for AMS Radiocarbon Preparation and Research in Boulder, Colorado.

The problem with radiocarbon dating marine organism is, that the turnover of oceanic water bodies is much slower than that of the atmosphere and therefore the deep waters are very old. When the surface water mixes with this old ^{14}C depleted deep water it affects the marine organism that live there (Bradley, 1985). Thus it is necessary to correct these ^{14}C dates with marine reservoir correction. The global average reservoir correction of about 400-year was applied to the ^{14}C dates for core A2010-10-5860.

Because of complexities in ocean circulation the actual correction varies with location. This regional difference from the average global marine reservoir correction is expressed as ΔR (Stuiver and Reimer, 1993). Studies north of Iceland show changes in the reservoir age over the past 3000 years (Larsen et al., 2002). There are no records available for ΔR in Arnarfjörður or nearby location. Studies from Scottish fjords (Cage et al., 2006) and Danish fjords (Heier-Nielsen et al., 1995; Olsen et al., 2009) show that freshwater input in fjords does effect the reservoir age and that the variability is high. There are several factors involved, such as the catchment size, water depth, fresh water supply and the dissolved terrestrial carbon which the freshwater brings into the fjord. Study from the Baltic Sea showed that the ΔR is affected by hydrographic conditions and local carbon inputs and is likely to significantly vary on spatial and temporal bases (Lougheed et al., 2013).

4 Foraminiferal ecology

Foraminifers are single-cell protozoa and live nearly exclusively in a marine environment. They are generally divided into two main groups: benthic, which live on the sea floor (epifaunal) or beneath the sediment (infaunal), and planktic, which float in surface waters (Murray, 1991). The soft cell builds a test for protection, either out of an organic membrane, agglutinated material or calcium carbonate ($CaCO_3$). Foraminifera has a wide environmental range, from terrestrial to deep sea and from polar to tropical (Murray, 1991). In fjords, foraminiferal assemblages are predominantly made up of benthic species due to unfavorable conditions for the planktic species, such as fresh surface layers and the dominant outward flow of surface water (Murray, 1991). Benthic foraminifera can be used as a climatic and paleoenvironmental proxy by quantifying the abundance, diversity and assemblage composition (Howe et al., 2010). In the deep ocean where physical factors are generally extremely stable biological factors such as food supply are often the major controlling factors for the benthic foraminifera distribution. In less stable marginal and shelf seas, physical and chemical factors are known to be important determining factors (Murray, 2001). The primary production is generally the main food source for benthic foraminifera, and the distribution of species on the shelf is related to the amount and type of organic supply, water mass characteristics, temperature and salinity.

Modern distribution studies of benthic foraminifera (Hald et.al., 1994; Hald et al., 1999; Korsun and Hald, 2000; Rytter et al., 2002; Jennings et al., 2004) have made it possible to distinguish between deep water and shallow water species, arctic and boreal species and species that live in brackish, saline or hyper-saline water. Rose Bengal has been widely used to differentiate living from dead foraminifera. Parameters influencing the foraminiferal ecology can be physical, chemical and biological, e.g. changes in temperature, water turbulence, current strength, salinity and primary productivity (Rytter et al., 2002). Many species are especially sensitive to environmental changes and are therefore useful in paleoecological and paleoenvironmental studies. Identifying benthic foraminiferal faunal composition is also a reliable tool to characterize glacial, deglacial and postglacial marine environments (Korsun and Hald, 2000).

4.1 Taxonomical comments

Out of the 36 foraminifera species identified in core A2010-10-586 only three were classified to family levels without being classified as species. Of the 66 samples analysed, 27 contained unidentified species.

Elphidium excavatum forma *clavata* and *Elphidium excavatum* forma *selseyense* were counted as one species due to difficulties in differentiating them. The arctic *E. excavatum* f. *clavata* can be distinguished by diminishing suture towards the middle while the boreal *E. excavatum* f. *selseyense* can be identified by lack of umbilical boss.

Similarly, *Stainforthia feylingi* and *Stainforthia fusiformis*, were also counted as one species due to similarities and difficulties to distinguish apart. *S. feylingi* has more of an elongated shape and is normally found in recent arctic to cold boreal environments

(Knudsen and Seidenkrantz, 1994), whereas the boreal *S. fusiformis* has a shorter and broader shape often with more distinct aperture. In core A2010-10-586 these two species are, however, not as common as *E. excavatum*.

Buccella calida and *Buccella hannai arctica* were counted separately but grouped as one species for transfer function calculations.

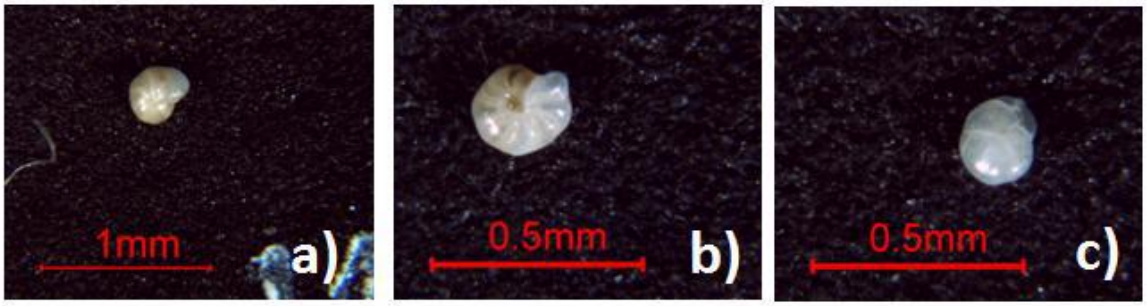

Figure 4-1: The three most common benthic foraminifera in core A2010-10-586. a) Cibicidis lobatulus, b) Elphidium excavatum and c) Cassidulina reniforme.

4.2 Ecology of selected species

***Astrononion gallowayi* Loeblich & Tappan**

A. gallowayi is an epifaunal species that can be found occasionally living infaunally (Murray, 1991). It is found in modern arctic environments, prefers temperature of < 1°C and is often found with *C. lobatulus* in relatively coarse sediments and where strong bottom currents persist (Polyak et al., 2002). Jennings et al. (2004) found *A. gallowayi* alongside *C. lobatulus* to be the most common species in Djúpáll, northwest of Iceland, in an environment dominated by strong bottom currents and coarse substrate. *A. gallowayi*, and *C. lobatulus*, are also the most common species along the North Icelandic coastline were the NIIC (bottom water temperature around 0.4° C– 4.1° C) dominates (Rytter et al., 2002).

***Buccella* sp.**

Buccella sp. is infaunal (Murray, 1991) and is most often found in an environment of muddy sediments, normal salinity and cold to temperate waters (Hald and Steinsund, 1996). The *Buccella* sp. is possibly linked to enhanced fluxes of food and sediment or seasonal sea ice. The species is also found to be motile, moving up and down in the sediment (Polyak et al., 2002). In Polyak et al (2002) *Buccella* sp. is described as a common species in the southern Kara Sea, possibly linked to coarser grained substrate and is often found in estuaries environment.

***Cassidulina reniforme* (Nørvang 1945)**

C. reniforme is an arctic infaunal spesies that favors muddy or sandy substrate (Murray, 1991). *C. reinforme* is found in cold-water areas (temperatures below 2 °C) with seasonal sea-ice cover (Polyak et al., 2002) and is often the most dominated species in modern glaciomarine environments (Hald and Steinsund, 1996). It is a small, opportunistic species

that can quickly respond to seasonal or pulsed organic matter supplies, it is resistant to oxygen deficiencies, and is often dominating in stressed, unstable environments such as soft bottoms close to glacial discharges (Korsun et al., 1995).

***Cibicides lobatulus* (Walker and Jacob, 1798)**

C. lobatulus is a cosmopolitan species and a suspension feeder. It is an epifauna, which attaches to rocks, plants or other substrates on the ocean bottom (Murray, 1991). *C. lobatulus* thrives in depths of 0 to more than 2000 m depth, but is most abundant on shallow banks (Murray, 1991). *C. lobatulus* is found in an area with coarse grained sediments and high energy regime (Klitgaard-Kristensen and Serjup, 1996). Temperature does not seem to be a limiting parameter for this species, but low salinity does, it prefers salinity >32‰ (Hald and Steinsund, 1996; Hald et. al., 1999).

***Elphidium albiumbilicatum* (Weiss, 1954)**

E. albiumbilicatum is infaunal boreal species (Rytter et al., 2002). It is often found in shallow environment and can tolerate reduced salinity, and is therefore a common first inhabitant after the transition from fresh- to brackish-water condition (Kristensen et al., 2000).

***Elphidium excavatum* (Terquem 1875) forma *clavata* (Cushman 1930) / forma *selseyense* (Heron-Allen og Earland)**

E. excavata f. *clavata* and *E. excavata* f. *selseyense* can be difficult to separate due to similar appearances but they live, however, in very different environments. *E. excavata* f. *clavata* is and arctic species but *E. excavata* f. *selseyense* boreal (Feyling-Hansen, 1972). *E. excavatum* f. *clavatum* is the most frequent shallow marine benthic foraminiferal species from late Quaternary glaciomarine deposits from high northern latitudes (Hald and Korsun, 1997). *E. excavatum* f. *clavata* is opportunistic and is adapted to deal with intense turbidity of glacial melt water outbursts and with ice proximal environments (Korsun and Hald, 2000). These environments are associated with rapid sedimentation rates and with harsh and variable conditions. *E. excavatum* f. *clavata* is often the first to colonize seafloor areas unfavorable for most life.

***Miliolinella subrotunda* (Montagu, 1803)**

M. subrotunda is an epifaunal species, which has been associated with the NIIC on the North Iceland Shelf (Rytter et al., 2002). The species is widespread on the inner shelf in slightly brackish to hypersaline lagoons (Altenbach et al., 1993)

***Stainforthia fusiformis* Williamson, 1858 / *feylingi* Knudsen & Seidenkrantz, 1994**

Both *S. fusiformis* and *S. feylingi* are infaunal species (Murray, 1991). *S. feylingi* is normally found in recent arctic to cold boreal environments but *S. fusiformis* is a boreal species. They are both considered opportunistic species and often associated with low-oxygen (Nordberg et al., 1999), and low salinity waters. *S. fusiformis* is often found in covariance with high seasonal productivity (Gooday and Alve, 2001). In the North Atlantic region *S. feylingi* has been recorded in arctic and subarctic waters from Greenland, Canada, Spitsbergen, the Norwegian continental margin, and the Arctic Ocean at water depths between a few meters and several thousand meters (Gooday and Alve, 2001). The

relatively high frequency of *S. feylingi* found in transitional zones reflecting change between arctic and boreal conditions may indicate that it is especially tolerant of unstable conditions (Knudsen and Seidenkrantz, 1994). In northern Europe it is common in shelf areas, coastal fjords and lower estuarine environments (Alve, 1990).

***Quinqueloculina stalkeri* Loeblich & Tappan, 1953**

Q. stalkeri is an epifaunal species (Murray, 1991), found in glacial marine environment (Korsun and Hald, 2000) and often in relatively shallow waters (< 50 m) (Korsun and Hald, 1998).

4.3 Statistical application

Successful reconstruction of past oceanographic conditions relies on reliable temperature proxy. Most commonly used are $\delta^{18}O$ measurements, since the oxygen isotopic composition of a foraminifera shell reflects the oxygen isotopic composition of the seawater in which the shell calcifies (Bradley, 1985). The $\delta^{18}O$ value is then converted to temperature, but with the assumption that the salinity has changed insignificantly in the past. In an attempt to disentangle the salinity signal from the temperature signal Mg/Ca measurements on foraminifera have been useful in some regions. To successfully reconstruct the temperature with this method a strong calibration curve is needed, however, this has proven difficult in studies from Icelandic water as in a near shore environment the isotope composition will be affected by freshening from runoff or melt-water. Therefore, when trying to reconstruct temperature changes from e.g. a fjord core, it is necessary to use other methods to estimate temperature and salinity.

4.3.1 Temperature and salinity reconstruction

The bottom water temperature (BWT) and salinity (BWS) reconstruction, in Arnarfjörður, were performed with transfer function applied to a down-core data set using the C2 program (Juggings, 2010). The transfer function is based on a calibration set by Sejrup et al. (2004), which presented a compilation of the distribution and abundance of recent benthic foraminifera (RBF) from the northwest European seaboard. The dataset includes benthic samples from shelf areas between 30 and 500 m water depths with 298 sediment surface-samples from northwest European and Iceland margin. The core site from Arnarfjörður falls within the geographical and physical frame of the RBF database, which allows reliable estimates of Arnarfjörður bottom water temperature.

The statistical routine, weighted averaging partial least squares (WA-PLS) was applied on the training set. In the database from Serjup et al. (2004) *E. excavatum* is included as one taxon because the participating researchers did not all identify them to subspecies level, even though the different subspecies of *E. excavatum* favor different ecological conditions. In arctic fjord environment *E. excavatum* f. *clavata* is fairly common specie due to its tolerance of high sediment accumulation rates and fluctuating salinity. To avoid the issue of too low temperature estimates, a square root was applied on the training set to diminish the weighing of *E. excavatum* on the temperature estimates (D. Klitgaard-Kristensen, personal communication). The average sample specific standard error for the temperature estimates is ±0.6704°C and for salinity ±0.0732 psu.

4.3.2 Cluster Analysis and Principal Components Analysis

Multivariate statistics programs (MVSP) perform several types of eigenanalysis ordinations, two of them being: principal components analysis (PCA) and cluster analysis (CA). To help with the interpretation of the foraminiferal faunal data from Arnarfjörður, both the PCA and CA were applied to the data set. In Core A2010-10-586 a total of 66 foraminiferal samples were analyzed. In the foraminiferal % dataset 17 species had ≥ 2% abundance in at least one sample.

The software Past was used for the cluster analyses. Results from species with abundance ≥ 2% were analyzed for the clustering. Squared Euclidian, paired group (UPGM) and constrained clustering were chosen when plotted (dendrogram), this allowed for the identification of zones for the foraminiferal fauna.

The PCA was used to better understand the association between foraminiferal assemblages and oceanic and environmental factors. The PCA was performed on the foraminiferal data set, with the XLSTAT software. The data set contained only species with an abundance of ≥ 2 % in at least one sample.

5 Results

5.1 Age model

The radiocarbon dates were converted to calendar years using the CALIB 7.0 Radiocarbon Calibration online program (http://calib.qub.ac.uk/calib/calib.html) with the MARINE13 data set (Reimer et al., 2013). There were no visual tephra layers found in the core A2010-10-586. However, two crypto-tephra fragments were found in the 63 and 106 µm sample sizes at the depth of 58 cm and 426 cm. Those samples were geochemically analyzed at the University of Iceland. The result for the upper tephra layer contains a mixture of several geochemical compositions which indicates reworked tephra rather than primary crypto-tephra. The geochemistry for the lower tephra showed a composition of Katla tephra (Table 5-1). According to the radiocarbon dates the tephra layer was deposited between ca. 350 – 1000 AD. For that time interval three known Katla layers (7^{th} century, 8^{th} century and 9^{th} century) have been found in marine sediments north of Iceland (Kristjánsdóttir et al., 2007; Guðmundsdóttir et al., 2012). All three tephra layers have a similar chemical composition which makes it hard to distinguish between them. However, based on the radiocarbon dates it was concluded that the oldest of these three Katla layers (~700 AD) was the one found in core A2010-10-586 and thus included in the age model (Table 5-2).

Table 5-1: The mean chemical composition of glass from the geochemical analysis of the crypto-tephra found in A2010-10-586 (n=number of analysis).

Tephra marker		**SiO_2**	**TiO_2**	**Al_2O_3**	**FeO**	**MnO**	**MgO**	**CaO**	**Na_2O**	**K_2O**	**P_2O_5**	**Total**
Katla 700 AD	Mean (n=14)	47.18	4.23	12.87	14.47	0.21	5.28	9.80	2.95	0.69	0.51	98.18

Table 5-2: Age model information from core A2010-10-586.

Depth (cm)	**Labrotory No.**	**Material**	**^{14}C age BP**	**^{14}C age range BP ±1sigma**	**Cal age AD (ΔR=0)**
36	CURL-16067	Marine bivalve shell	555	20	1756
164	CURL-16081	Marine bivalve shell	905	20	1437
305	CURL-16073	Marine bivalve shell	1395	20	1002
426		Katla tephra			~700
512	CURL-16078	Marine bivalve shell	2020	20	356

The chronology in core A2010-10-586 is based on the four AMS radiocarbon dates and one crypto-tephra layer (Table 5-2 and Fig. 5-1). The sediment accumulation rate was calculated by linear interpolation between the dated levels. The bottom part of the core has the lowest sedimentation rate of 2.5 mm/yr. From ca. 700 to 1000 AD the sedimentation rate increases to 4.0 mm/yr, than it decreases and stays fairly stable around 3.2 – 3.9 mm/yr towards the top.

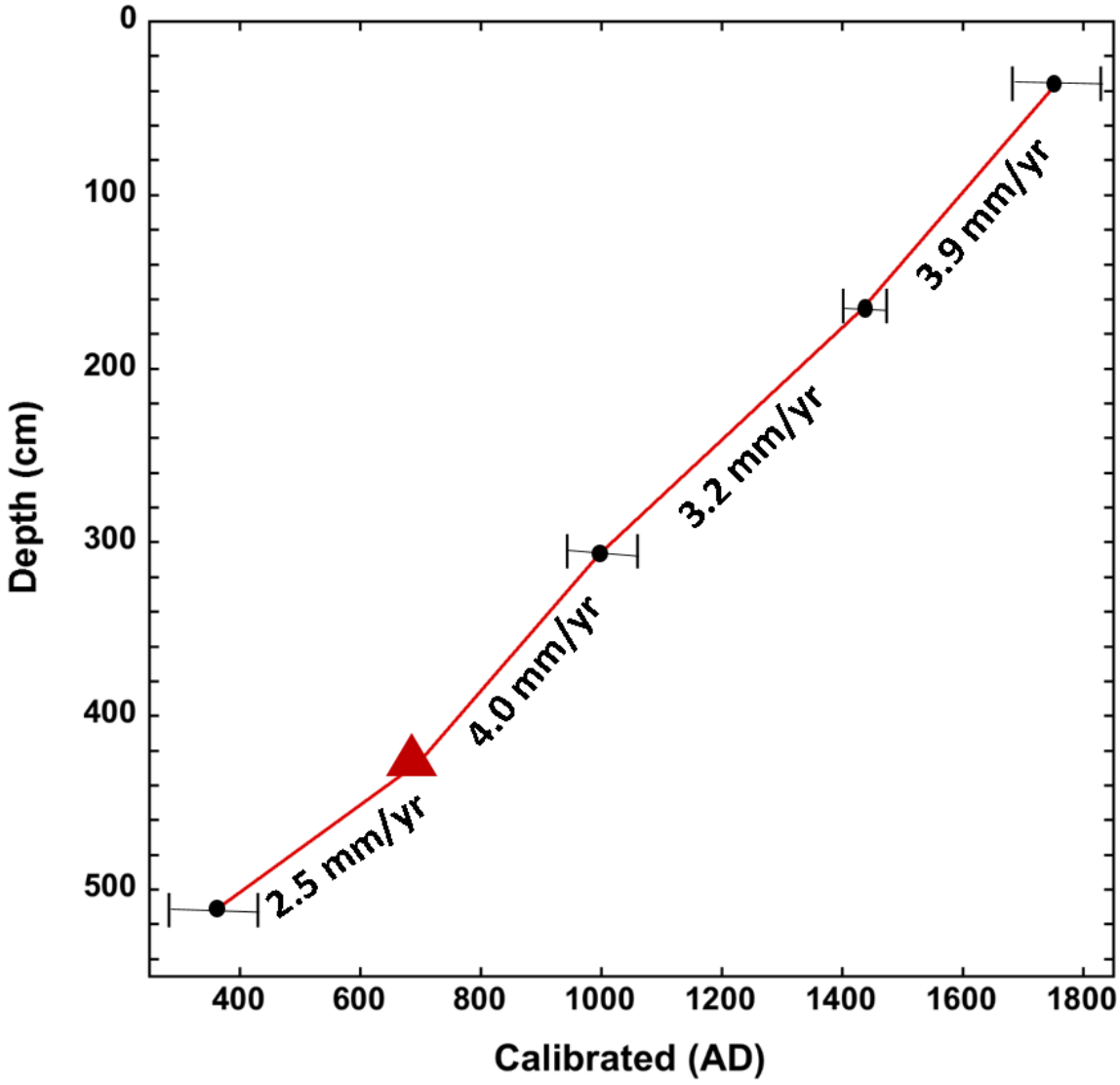

Figure 5-1: Age-depth model for core A2010-10-586, based on four ^{14}C AMS date. The depth of the Katla tephra was incorporated into the age model and is indicated by red triangle.

5.2 Lithology and sedimentology

Core A2010-10-586 was split into five core units (A-E) (Fig. 5-2). Apart from unit E, no clear changes in color or structure could be seen by the naked eye. The x-rays, however, showed some changes in the grain size, with much finer grain size for the bottom part (ca. 350-900 AD) compared to the upper part of the core (Fig. 5-2). The lower part of the core also contained more abundance of mollusks compared to the upper part. The location of mollusks retrieved for ^{14}C analysis, the Katla tephra layer along with lithological information are demonstrated in figure 5-2. Around ca. 1000 AD pebbles start to increase in the core. The top 30 cm of the core (unit E) covering the time interval from ca. 1600 to 1850 AD was much darker and more liquid than the older part of the core

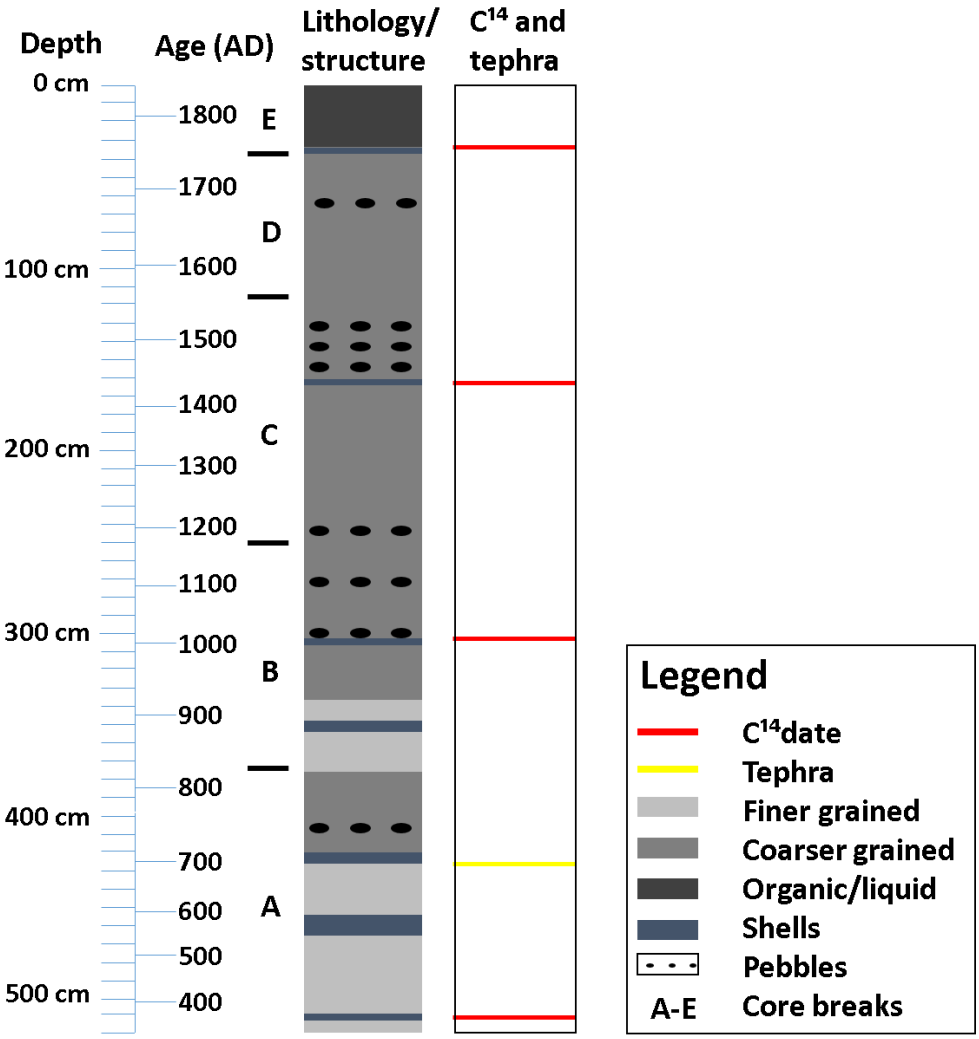

Figure 5-2: Simplified drawing of structure and lithology in core A2010-10-58

5.3 Physical and organic properties of the sediments

5.3.1 Magnetic susceptibility

The MS values for the bottom part of the core (350-550 AD) are fairly stable with values from ca. 20-40*10^{-5} SI (Fig. 5-3). There is a peak in the measurements around 600 AD where the values reach ca. 60*10^{-5} SI, and a broader peak around 700 AD with ca. 50*10^{-5} SI. At ca. 950 AD the MS increases, reaching ca. 70*10^{-5} SI. One of the lowest values (10*10^{-5} SI) was measured around 1150 AD. From ca. 1250 – 1400 AD the values decrease from ca. 50*10^{-5} SI down to 15*10^{-5} SI. The MS for the top part of the core (1400–1850 AD) shows fluctuations between the highest measured MS (78.9*10^{-5} SI) and the lowest measured values (10*10^{-5} SI). The MS record shows two broad peaks, at 1050 AD and again between 1650 and 1750 AD with the highest value of 79.8*10^{-5}SI. The top part of the core (upper most 30 cm) is more liquid, than the rest of the core, which may have affected the measurements. The average value is 34.7*10^{-5}SI.

5.3.2 Density

The density shows strong covariance with the MS reconstruction (Fig. 5-2). It is fairly stable from 350-1000 AD with values around 1.9 g/cc. At approximately 1200 AD the density values show increased fluctuation. The values start to decrease around 1450 AD with the lowest one at ca. 1550 AD (1.54 g/cc). After that the density increases until ca. 1750 AD when the values drop and stay fairly low to the top part of the core. The mean value is 1.939 g/cc, with the highest value being 2.04 g/cc and the lowest being 1.54 g/cc.

5.3.3 X-ray radiographs

Every cm was examined on the radiographs and pebbles larger than 2 cm in diameter where counted. No IRD was detected in the finer grained bottom part of the core between 350 and 700 AD (Fig. 5-3). At ca. 750 AD the first sign of coarser material in the core is found increasing between 1000 and 1150 AD. A significant change towards coarser grain sizes is apparent around 1100 AD. The most abundant IRD is between ca. 1250 and 1300 AD and again between ca. 1450 and 1600 AD. The top part of the core between 1600 and 1850 AD shows considerable variations in the amount IRD.

5.3.4 X-ray diffraction (XRD)

The results from the XRD measurements indicate little or no quartz in the sediment core (Fig. 5-3). The highest value measured was 3 wt% and the overall trend shows a decrease towards the top of the core. The carbonate data, however, shows more changes in its wt%. The bottom part of the core, from ca. 350 AD – 800 AD, has fairly stable content of carbonate although steadily increasing. Around 900 AD the carbonate values decrease and reach a low around 1050 AD. After 1200 AD the values start to increase towards the top of the core but show a distinct low in the measurements between ca. 1550 and 1750 AD. The lowest value for the carbonate was 17 wt% (ca. 1000 AD) and the highest of 24 wt% (ca. 1800 AD).

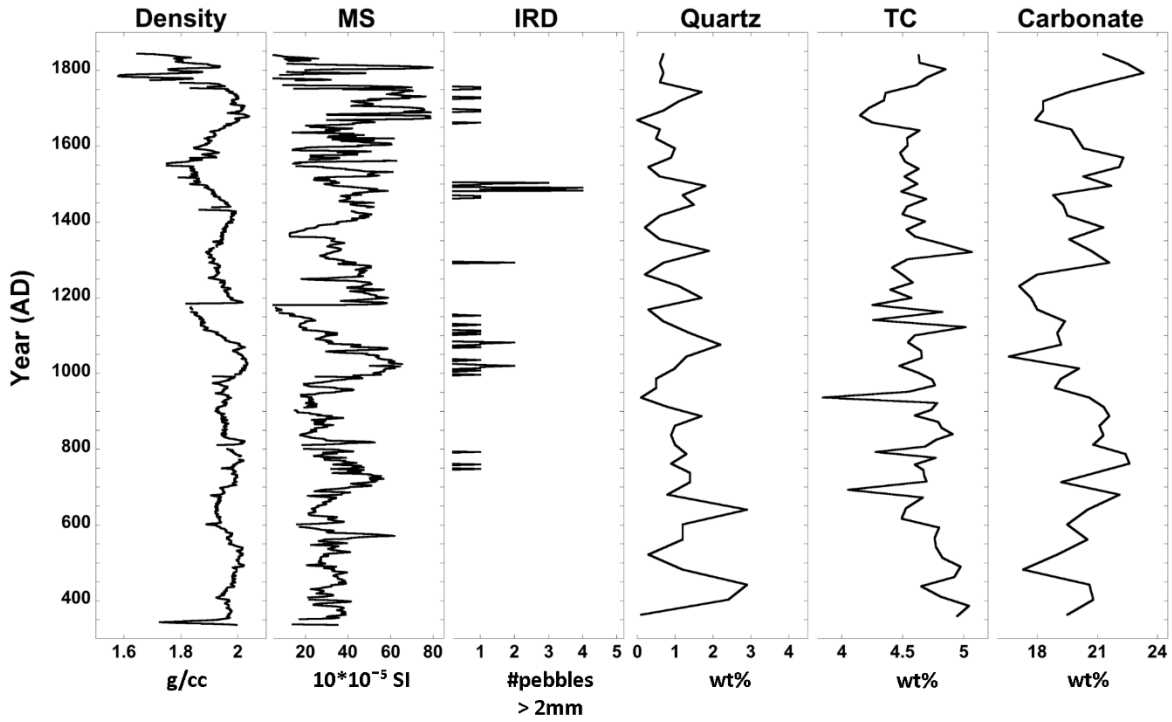

Figure 5-3: Physical and organic proxies from core A2010-10-586. Density and MS measurements represent changes in the grain size and the amount of terrestrial material in the core. IRD shows intervals with pebbles > 2mm in the core. The Quartz is a measure of drift ice, the TC shows changes in the organic material and the carbonate is a measure of surface water stratification and nutrient supply.

5.3.5 Total Carbon

The TC% record from A2010-10-586 shows an overall decreasing trend towards the top of the core, where the bottom part has higher and more stable values (Fig. 5-3). The highest TC% of 5.07 wt% is measured at ca. 1300 AD, after that the values slowly decrease. Between ca. 1650 and 1700 AD is a distinctive low in TC%. The TC% in the upper part of the core, from 1700 AD to the top (1850 AD) fluctuate between 4.3 - 4.7 wt%. The median TC% value is 4.63 wt%.

5.4 Foraminiferal analyses

In core A2010-10-586 a total of 37 benthic foraminifera species were identified (table 5-3), including one agglutinated species. The diversity of the individuals ranged from 8 – 24 in each sample. The three most dominant species were *C. lobatulus, C. reniforme and E. excavatum* (55.7% - 90.7%). Planktic foraminifera was present in 19 out of the 66 samples from the core.

Table 5-3: List of all the calcareous species found in core A2010-10-586.

Astrononion gallowayi	Loeblich & Tappan, 1953
Bolivina pseudopunctata	Höglund, 1947
Bolivina skagerrakensis	
Buccella calida	Cushman and Cole, 1930
Buccella frigida	(Cushman, 1922)
Buccella hannai arctica	Voloshinova, 1960
Buccella tenerrima	(Bandy, 1950)
Cassidulina obtusa	Williamson, 1858
Cassidulina reniforme	Nørvang, 1945
Cibicides lobatalus	(Walker & Jacob, 1798)
Cibicides pseudoungerianus	Cushman, 1982
Cibicides refulgans	de Montfort, 1808
Cyclogyra involvens	(Reuss, 1850)
Dentalina sp.	
Discorbis nitidae	
Elphidium albiumbilicatum	(Weiss, 1954)
Elphidium excavatum	Terquem 1875
Elphidium spp.	
Epistonella spp.	
Fissurina laevigata	Reuss, 1850
Glabratella arctica	Scott og Vilks 1991
Globobulimina auriculata arctica	(Bailey, 1894)
Islandiella helenae	Feyling-Hanssen & Buzas, 1976
Islandiella norcrossi	(Cushman, 1933)
Lamarckina halitidea	Heron-Allen & Earland, 1911

Table 5-3 continued

Milliolinella subrotunda	(Montagu, 1803)
Nonionella turgida	(Williamson, 1858)
Nonionella auricula	Heron-Allen & Earland, 1930)
Oolina melo	d'Orbigny, 1839
Patellina corrugata	Williamson, 1858
Pullenia osloensis	Feyling-Hanssen, 1954
Pyrgo williamson	(Silvestri, 1923)
Quinqueloculina seminulum	(Linné, 1758)
Quinqueloculina stalkeri	Loeblich & Tappan, 1953
Rosalina villardeboana	d'Orbigny, 1839
Stainforthia feylingi	Knudsen & Seidenkrantz, 1994
Stainforthia fusiformis	Williamson, 1858

5.5 Statistical results

5.5.1 Cluster Analyses

Constrained Cluster Analyses (CA) defined three assemblage zones from top to bottom (1 to 3) and two subzones (Fig. 5-4). The CA results are presented in a dendrogram, showing three distinct groupings. The first group covers the interval from 350 to ~800 AD, the second group is from ~800 to 1200 AD and the third one from 1200 to 1855 AD. The last group is divided into two subzones, one from 1200 to 1350 AD and the other from 1350 to 1840 AD.

Zone 1: 350-800 AD.

C. lobatulus dominates this zone with up to 76.6% of the individuals in the bottom samples (Fig. 5-5). The Arctic species *C. reniforme* and *E. excavatum* f. *clavata* show low values (5-10%) near the bottom part, increasing up to ca. 60% at around 500 AD. Conversely, *C. lobatulus* decreases over the same interval. After that *C. reniforme* decreases towards the upper part of this zone but *E. excavatum* values continue to increase. *A. gallowayi* is fairly stable throughout the zone with ca. 3-8% of the faunal composition. *Q. stalkeri* shows 7% at the lower part of the zone but decreases near the top. *B. calida* shows fluctuating abundance (1-4%) in this zone. Other species do not have high abundance. The diversity of the foraminiferal sample range froms 11-19 in each sample.

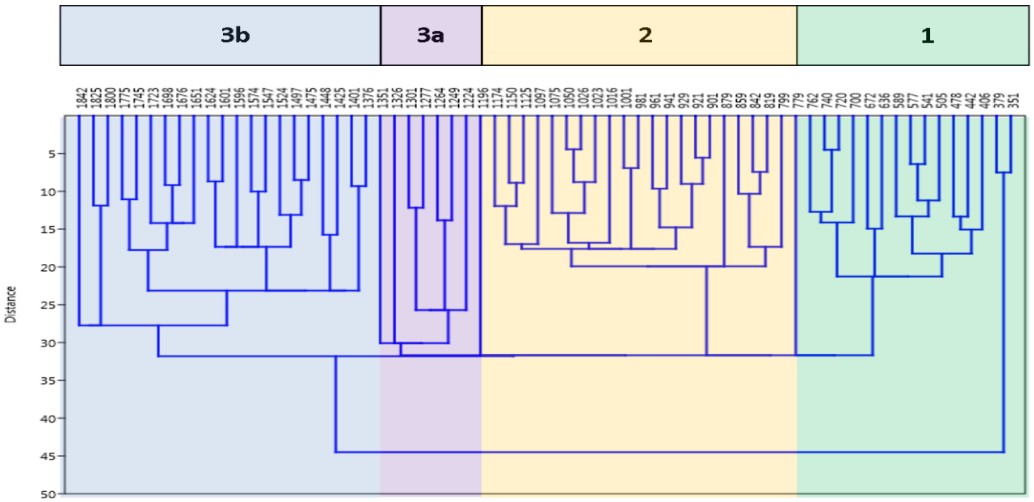

Figure 5-4: Dendrogram. Clustering analysis was performed on the original data set containing all foraminifera species found in the core.

Zone 2: 800-1200 AD

In this zone *C. lobatulus* still dominates with up to 59% of the faunal composition. *E. excavatum* peaks (41.1%) at the lowest part of this unit but then it decreases in abundance, having its lowest value around 1000 AD (Fig. 5-5). *C. reniforme* slowly increases from 15% up to 40%. Both *A. gallowyi* (11.5%) and *B. calida* (5.4%) peak in this unit. *B. hannai arctica* increases from ~1% up to 4.5% at the top of the unit. *Q. stalkeri* has a sudden increase (11.2%) in one sample near the upper part of this zone and *Q. seminulum* peaks (5.4%). *F. leavigata* and *S. fusiformis/feylingi* are 2.5% near the lowest part of this unit fluctuating upwards although not reaching high abundance. The diversity ranges from 10-19 species in each sample.

Top Zone 3: 1200-1845 AD

Subzone 3a: 1200-1350 AD

This subzone spans the shortest intervals of only ca. 150 yr (Fig. 5-5). There are however couple of species that peak during this interval. *C. lobatulus* is fairly stable with ca. 25-50% of the faunal composition. *C. reniforme* decreases, though reaching 30% at the upper part of this zone. Both *E. excavatum* (15% - 33%) and *Q. stalkeri* (~5%) show an increasing trend in this zone. *B. hannai arctica* (10.8%) and *B. frigida*, show a distinct increase, reaching their highest abundance in the core in this subzone. In this zone the highest diversity is found with 24 species (1264 AD), the other samples have around 12-16 species per sample.

Subzone 3b: 1350-1845 AD

In this subzone the most dominant species is *C. reniforme* (53%) along *E. excavatum* (25%). *C. lobatulus* decreases towards the top, fluctuating from 50% down to 8% (Fig. 5-5). At the top of this unit *Q. stalkeri* peaks (11.4%). The diversity in this zone ranges from ~10-20 individuals but three samples have the lowest count of only 8-9 individuals in each sample.

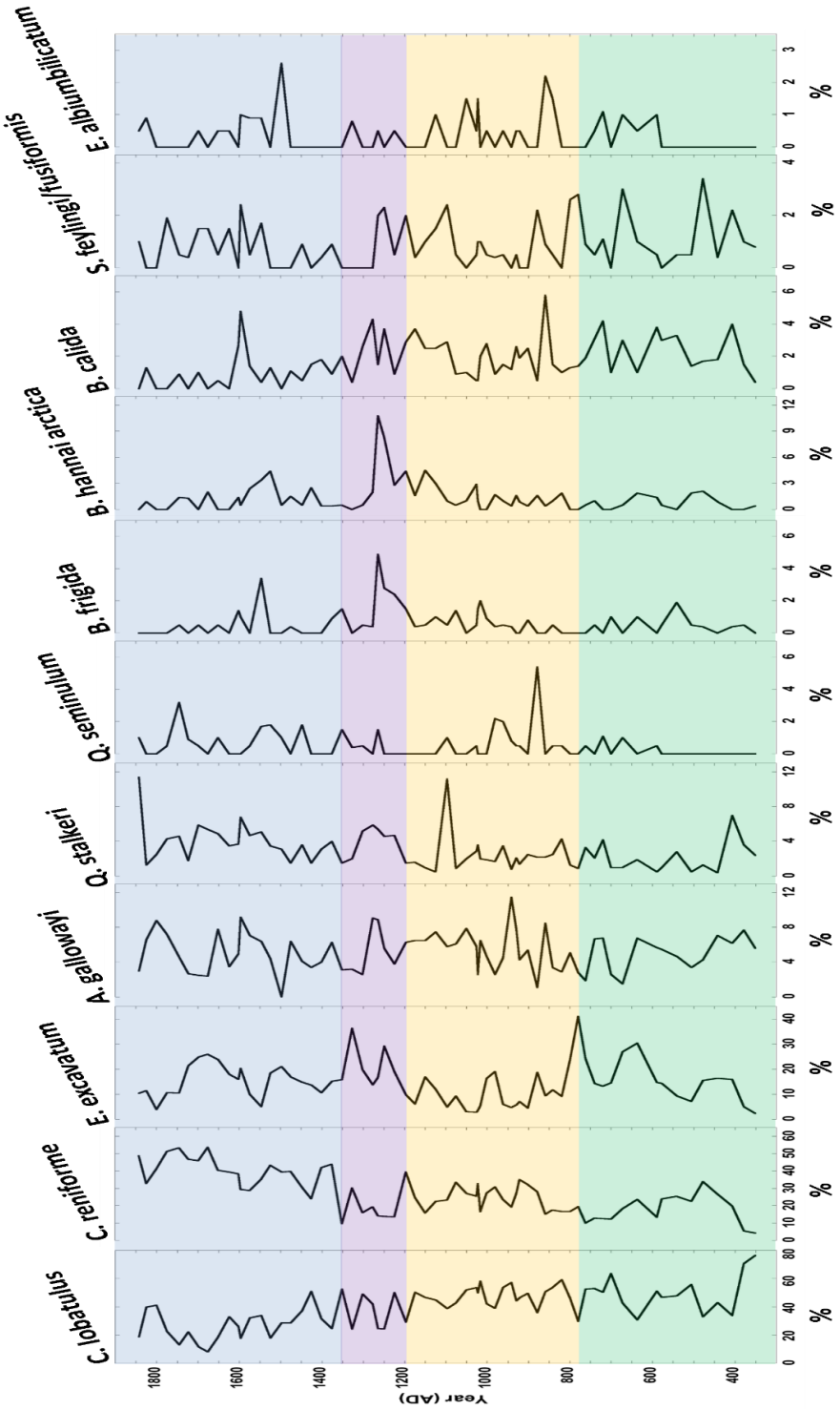

Figure 5-5: Foraminiferal abundances in core A2010-10-586. Shown here arespecies with 3% abundance or higher. The different colors indicate different foraminiferal zones.

5.6 Transfer function

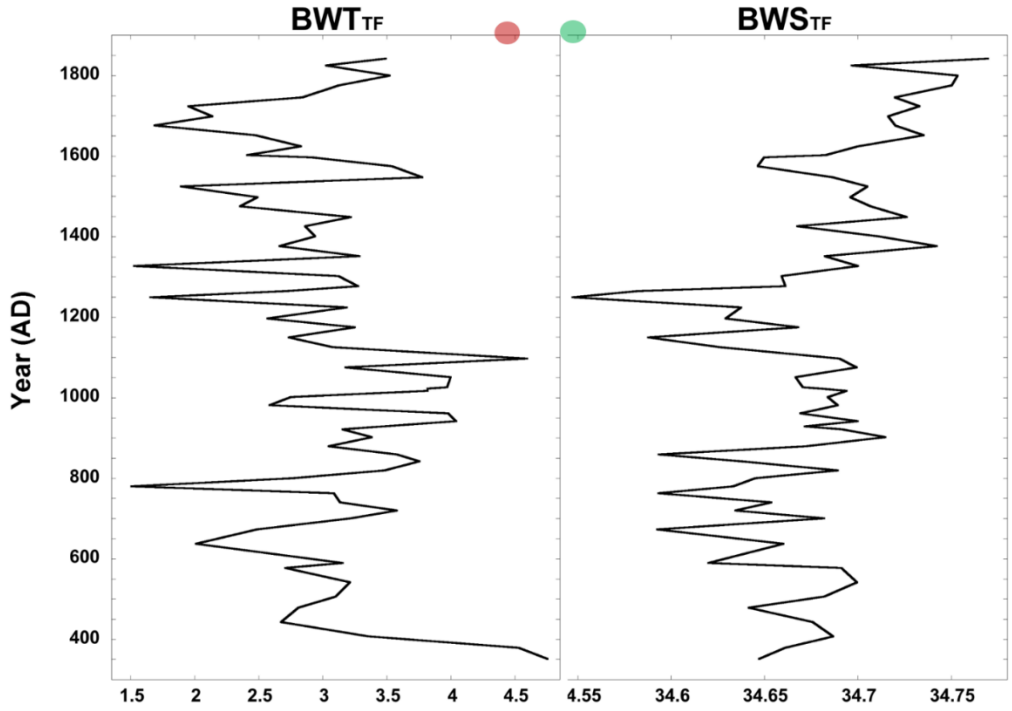

Figure 5-6: Estimated BWT and BWS in Arnarfjörður, based on transfer function analyses. The red dot represents the mean annual bottom water temperature in Arnarfjörður today and the green dot the mean annual salinity today.

The BWT_{TF} estimates range from 1.5°C to 4.75°C, a range of ~3°C, for the past 2000 years (Fig. 5-6). The temperature estimate is highest around 350 AD but decreases steadily until it reaches one of its lowest values around 800 AD. An interval of increased but fluctuating temperature is seen from 800 to 1100 AD. After that the temperature starts to decrease towards the top with distinctive lows around 1300, 1500 and 1700 AD.

The salinity reconstructions do not show as much variability as the temperature values, although fluctuating from 34.77‰ (highest value) to 34.547‰ at the lowest (Fig. 5-6). The values at the bottom part of the core at 350 AD fluctuate but with an increasing trend, from ca. 34.6 – 34.7‰ until around 500 AD. The values decrease slightly and stay stable from ca. 900 – 1100 AD. The salinity reaches the lowest value at ca. 1250 AD. After that the estimated salinity, unlike the estimated bottom water temperature, shows increasing trend upwards and peak at the top of the core.

6 Discussion

6.1 Interpretation of the Principal Component Analysis

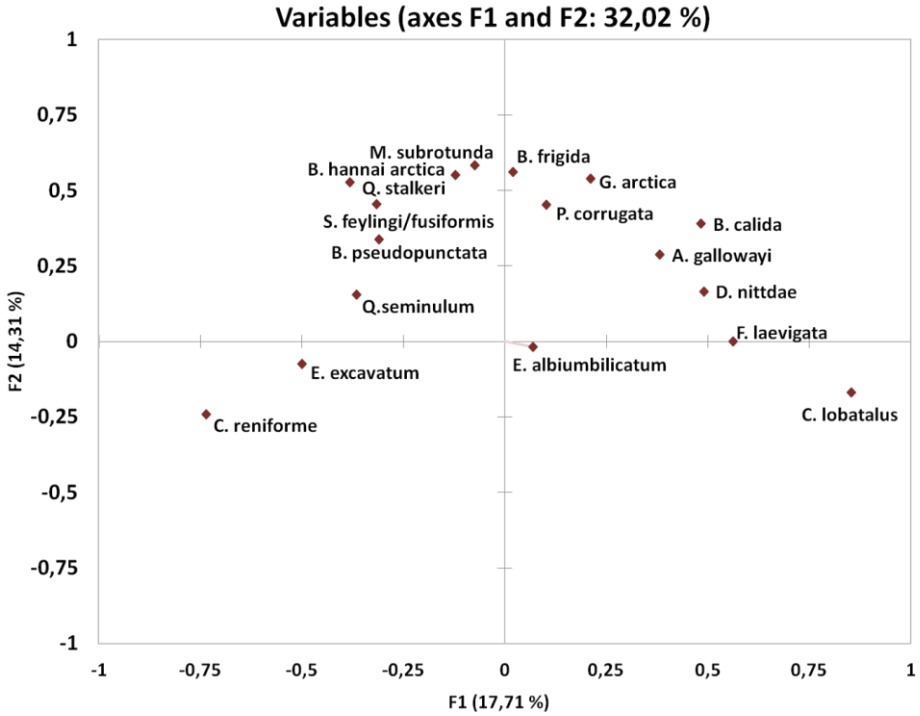

Figure 6-1: Scatter plot of species loadings on axis 1 and axis 2 from the Prinipal Component Analysis (PCA).

A linear method of PCA was used to identify statistically significant directions of variation within the samples. The first two axis accounted for 32% of variation for the benthic foraminifera (Fig. 6-1). The species that are negatively loaded on axis 1 (F1), *E. excavatum* and *C. reniforme* are known to live in Arctic (colder) water. Positively loaded on axis 1 is *C. lobatulus*, which is often linked to coarser grained substrate and stronger bottom currents. Stronger bottom currents could possibly be an indicator of a stronger flow from the Irminger Current. PCA axis 1 thus divides the species to Arctic water (negative loadings) and warmer waters (positive loadings). Negatively loaded on axis 2 is *E. albiumbilicatum*, often found in shallower sites with lower salinity than normal. Positively loaded on axis 2 are species associated with normal salinity such as: *M. subratunda*. *B. frigida, B. hannai arctica* and *G. arctica*. Even though it is impossible to rule out other factors like changes in food supply, the loadings on axis 2 (F2) are interpreted to represent salinity changes from less saline (negative loaded) to higher salinity (positive loaded).

6.2 Temperature and salinity reconstruction

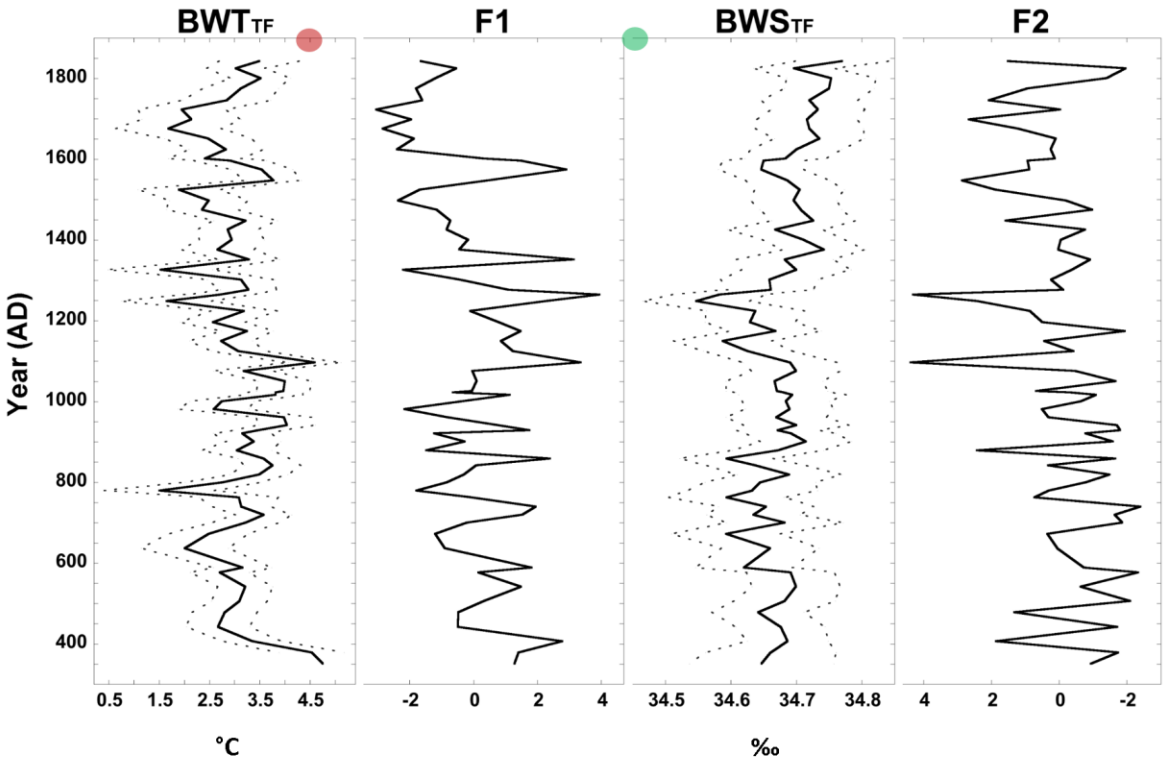

Figure 6-2: The BWT_{TF} and BWS_{TF} compared to the factor scores of axis 1(F1) and axis 2 (F2) from the PCA. The red dot represents the mean annual BWT in Arnarfjörður today and the green dot the mean annual BWS today. The sample specific standard error is marked with dotted lines.

Clear similarity is apparent when comparing the transfer function inferred temperature estimations with the factor scores from the PCA loadings (Fig. 6.2). Axis 1 in the PCA shows cold water species on the negative side but species that are found in environment with stronger bottom currents on the positive side. This could be interpreted as an indication of an increasing strength of the Irminger Current which brings warmer waters towards Iceland. The mean annual bottom water temperature in Arnarfjörður today is ~ 4.5°C (Fig 2-7). The estimated bottom water temperatures shows similar temperature values for the bottom part of the core and around 1100 AD. The values decrease towards the top of the core.

The salinity profile, however, does not show as strong similarity with the factor scores for axis 2. The similarity between the salinity and the factor scores are strongest in the lower part of the core but around 1200 AD with increasing salinity towards the top of the core the factor scores and salinity diverge from each other. When comparing the transfer function inferred salinity estimates to the present day values for Arnarfjörður the estimated ones are somewhat higher, and the modern values do not fall within the standard error of the estimated salinity values (Fig 6-2). This indicates that the modern data set used for the calibration does not capture the real salinity conditions in the fjord. It is evident that more research is needed on salinity change, especially in a fjord environment, and thus it was decided to discard the salinity profile.

6.3 Climate variability in Arnarfjörður for the past 2000 years: proxies interpretations

The core was divided into three units based on the cluster analysis (Fig. 5-3). The first interval (zone 1) comprises the bottom part of the core from ca. 350 to 800 AD and the second interval (zone 2) covers the time interval from ca. 800 to 1200 AD. The last interval (zone 3) covering the time from ca. 1200 AD to the top of the core (ca. 1850 AD) was divided into two subzones. The first one, subzone 3a, only spans ca. 150 years and was incorporated to subzone 3b.

6.3.1 Dark Ages Cold Period (DACP)

The oldest interval from the core spans the time period from 350 - 800 AD. The bottom part of this interval has the highest estimated temperature of the entire core (~ 5°C) with *C. lobatulus* as the dominant specie. High abundance of *C. lobatulus* often indicates stronger bottom water currents. The overall trend of the bottom water temperature shows a stepwise decrease throughout this interval with increasing abundance of the arctic species

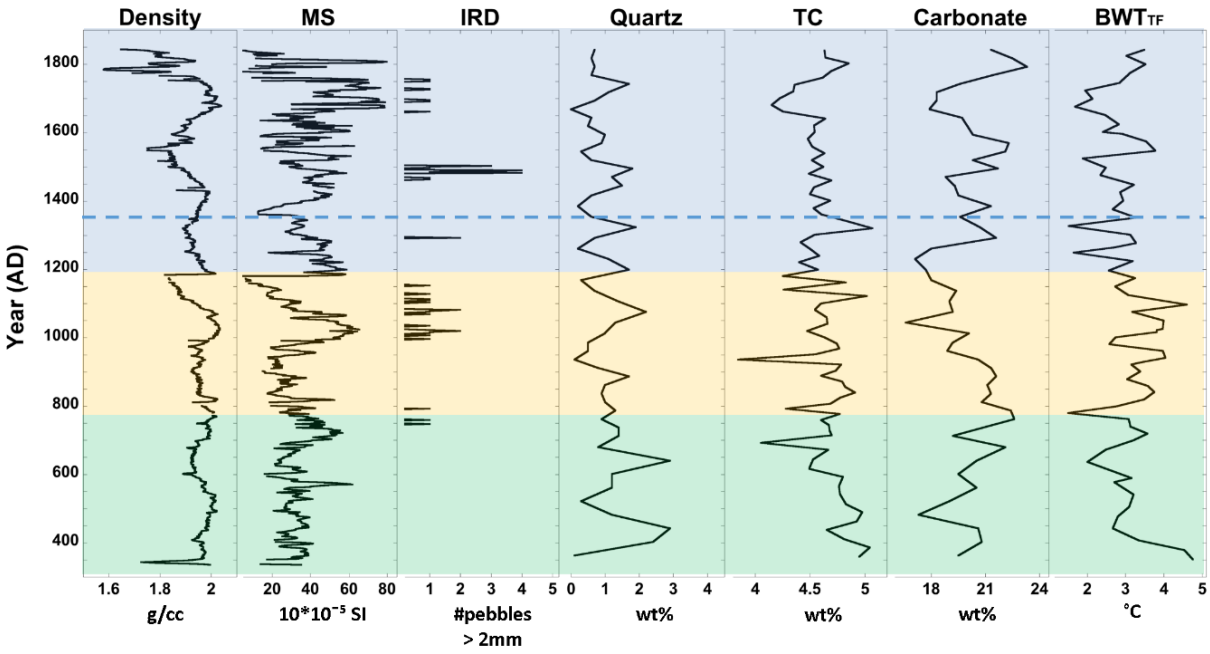

Figure 6-3: Proxy records from Arnarfjörður. The different colors represent three different periods based on the cluster analysis. The dashed line shows the boundaries between subzone 1a and 1b.

C. reniforme and *E. excavatum*, indicating increasing influence of colder currents in Arnarfjörður. The time period from 350 – 700 AD has the lowest sedimentation rate of ca. 2.5 mm/yr. At ca. 700 AD the sedimentation rate increases to 4.0 mm/yr. The overall trend of the MS values stays fairly stable throughout this interval, apart from a short increase around 550 AD, which could possibly be a tephra layer, and a broader increase around 750 AD. The density values show little fluctuation, which means that there are little changes in the grain size for this interval. That is also evident on the x-rays, which show fine grained

sediment with no IRD present. The total carbon percentage shows decreasing values upwards, which could suggest a decrease in bioproductivity. However, due to lack of information on the total inorganic carbon it is unclear what this decrease in TC indicates.

6.3.2 Medieval Warm Period (MWP)

This is the shortest of the three intervals in the core (800-1200 AD). For this part of the core the most noticeable changes in the foraminifera is the abrupt decrease of *E. excavatum*. Both *C. lobatulus* and *A. gallowayi* show increasing values at the beginning of this interval and stay fairly stable throughout it. The bottom water temperature derived from the foraminifera show increasing values for this interval with the highest temperature of ca. 4.5°C around 1100 AD, which is similar to the mean annual BWT in Arnarfjörður today. From 800 – 1000 AD the sediment is fine grained with no detectable IRD and low values of both density and MS (Fig. 6-2). At around 1000 AD there is an obvious change in the environment, with a rise in the MS and density values and coarser grained material is detected more frequently on the x-radiographs. Usually, the presence of IRD (coarser material) in sediment cores is linked to colder conditions. However, in a fjord environment the coarser grained material can also represents more eroded terrestrial material from the drainage area. Trouet et al. (2009) showed that the MWP, also known as the Medieval Climate Anomaly (MCA), was characterized by the NAO in its positive mode. During a positive NAO phase (Fig. 2-4) the Northern Europe and Iceland receives more precipitation (Hurrel, 1995), the influence of the Irminger Current is stronger on the North Icelandic Shelf and the northerly winds decrease. With more precipitation over Iceland the runoff from land increases and the rivers carry more terrestrial material to the sea. Increasing strength of currents could also have produced stronger tidal waves resulting in more material being eroded from the coast and that way brought more material into the fjord.

The carbonate values from Arnarfjörður are mostly composed of calcite, which is not thought to have a terrestrial source. Between 1000 and 1200 AD the carbonate wt% in Arnarfjörður reaches its lowest point. The lower values in the core might be reflecting the increasing sediment accumulation rate, which, according to the calculated sedimentation rate from the age model, increases a bit around 800 AD. Another explanation for this decrease in wt% carbonate is increasing in stratification of the water column, due to increase precipitation and runoff, which would, reduce the nutrient availability. In other words, during times when more run-off water is entering the fjord the nutrient supply would diminish and the carbonate wt% decrease.

6.3.3 Little Ice Age (LIA)

The bottom water temperature in this interval shows a significant decrease (of about 1°C) from the previous interval. The Arctic water indicators *E. excavatum, Q. stalkeri* and *Buccella* sp. (all of them are linked to ice proximal environment) start to increase around 1200 AD. Subzone 1a from the cluster analysis is possibly indicating a transitional zone when the faunal composition in the fjord starts to changes towards colder conditions. The time period from 1200 - 1400 AD indicate cooling but fairly stable conditions, with the MS values decreasing, suggesting less terrestrial material being deposited into the fjord. The x-rays show little or no IRD and the TC increases. The carbonate records from Arnarfjörður show a short-term increase, which can be linked to less stratification and more food supply. At the same time there is a short increase in the diversity of the foraminiferal fauna.

Around 1450 AD there are changes in the record. The estimated bottom water temperature drops down to ca. 2°C, with a change in the foraminiferal fauna. *C. lobatulus* decreases and *C. reniforme* becomes the dominant specie in the fjord. This is also the time when other proxy records in the fjord start to become more unstable. The MS record shows fluctuating values and the x-rays show higher abundance of IRD in the core. There is a peak in the IRD at ca. 1450-1500 AD which lines up with a drop in the bottom water temperature estimations. At approximately 1500 AD the bottom water temperature increases again, with a decrease in the arctic specie *E. excavatum.* There is no IRD detected in the core but the MS values shows, however, fluctuating values.
The interval between ca. 1650-1750 AD (Fig. 6-4) shows defined changes towards harsher conditions in Arnarfjörður with a drop in the bottom water temperature, TC and the carbonate values and at the same time the Arctic water species indicators *E. excavatum*, *Q. stalkeri* and *C. reniforme* increases. *E. excavatum* adapts easily to a wide range of environmental conditions, but often blooms during extremely cold and unstable conditions (Hald et al., 1994). In this interval the bottom water current indicator *C. lobatulus* has its lowest values and the diversity of the foraminifera fauna also reaches a low.

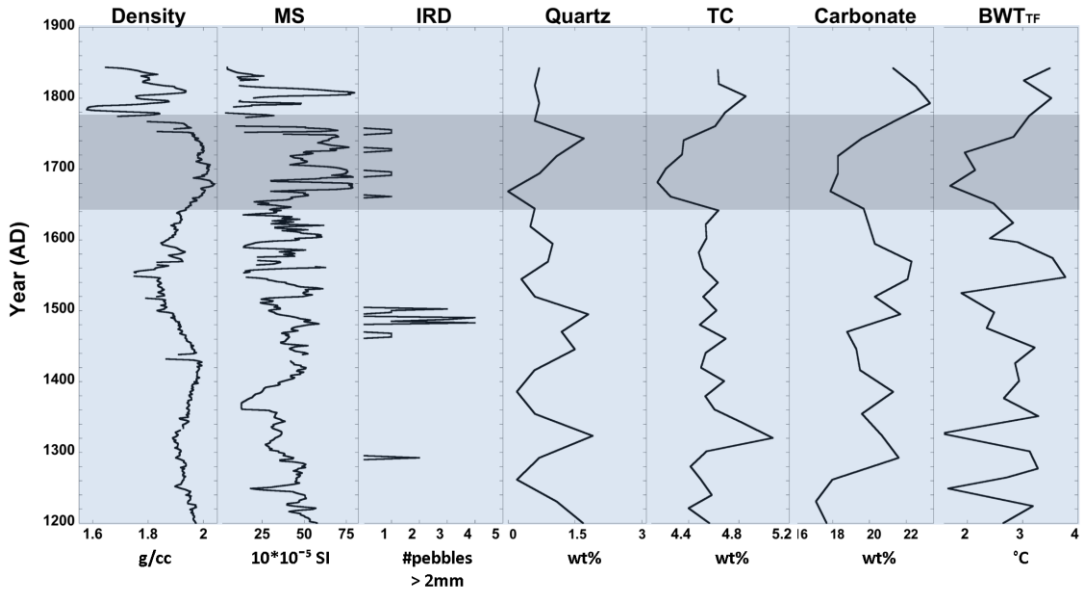

Figure 6-4: The proxies from core A2010-10-586 zoomed into the time interval between ca. 1200-1850 (LIA) . The blue band (ca. 1650-1750 AD) shows interval of harsh conditions in Arnarfjörður.

Colder conditions in the fjord are also evident by an increase in both density and MS values as well as increased amount of IRD. The coarser grained material found in Arnarfjörður after 1200 AD is not believed to have a distal source. Quantitative XRD analysis of the sediments in Arnarfjörður found no or little quartz (Fig. 6-2). Icelandic bedrock consists of basalts with quartz only found in low abundances, whereas sediment from western Greenland contains quartz (Andrews and Jennings, 2014). Quillmann et al., (2010) came to the same conclusion for core MD99-2266, from Ísafjarðardjúp, for the deglacial time. The most likely explanation of those IRD peaks are thus eroded material from the coast of Arnarfjörður.

6.4 Climate variability in the North Atlantic region during the past 2000 years

In recent years a number of studies have focused on climate reconstructions during the last two millennium in the North Atlantic (e.g. Andrews and Jennings, 2014; Geirsdóttir et al., 2009; Knudsen et al., 2012; Massé et al., 2008; Sicre et al., 2008). Many of these reconstructions have high (annual to decadal) resolution and exact dating, which allows the proxy records to be calibrated against instrumental data. Comparison with other proxy archive from the same region reveals considerable similarities in climate variability. Sediment cores from fjords tend to contain high resolution data as they act as sediment traps for terrigenous sediments eroded from the fjord drainage basins. They can be regarded as a link between the open ocean and land, where runoff from land mixes with ocean water, and thus potentially linking the different components of the climate system.
The main focus here is to look at the transition from the MWP to the LIA, the timing of that transition and changes in climate variability during the LIA. The MWP-LIA transition in the core from Arnarfjörður is found to be around 1200 AD when there is a defined change in the foraminifera faunal assemblage. Other high-resolution studies around Iceland and the North Atlantic show a similar trend, though the ages of boundaries between individual periods vary regionally

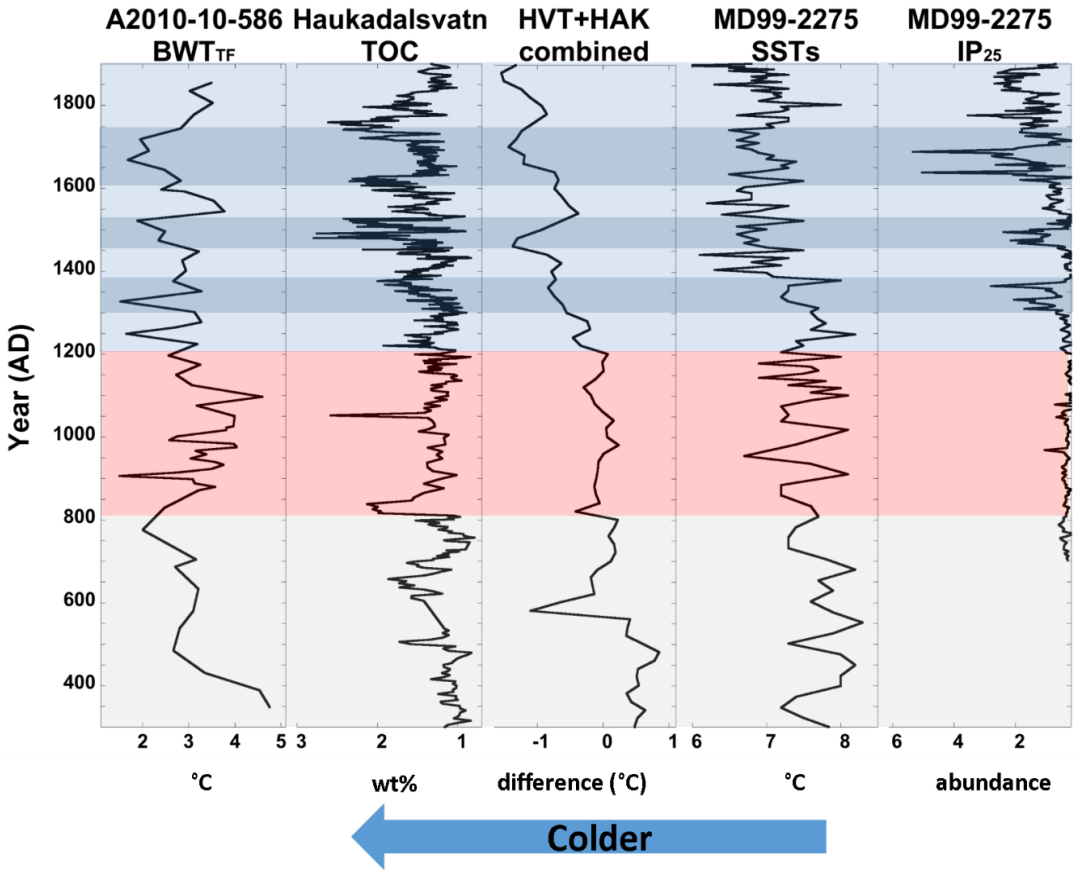

Figure 6-5: BWT of Arnarfjörður compared to TOC and combined proxies from Hvítárvatn (HVT) and Haukadalsvatn (HAK) (Geirsdóttir et al. 2013), Sea Surface temperatures (Sicre et al. 2008) and IP25 index (Massé et al. 2009) from core MD99-2275, north Iceland (note that the sea ice index and TOC has been inverted so that it trends in the same direction as the other records).

6.4.1 NW Iceland – Greenland

High resolution studies around the NW Iceland Shelf (Andrews et al., 2009) suggest a simple two-fold division in climate conditions over the last 1700 yr with the major change occurring at ca. 1200 AD. Andrews and Jennings (2014) compared records from sediment cores on the either side of the Denmark Strait, focusing on the trends of the weight% of calcite and quartz. Both sides showed a major environmental shift occurring ca. 1450 AD. The records from Arnarfjörður start to show more unstable conditions around that time. Study of the variability of the Irminger Current throughout the Holocene show a clear change, during the LIA, towards more unstable environment (Ólafsdóttir et al., 2010). In Reykjarfjörður, a small silled fjord in northwest Iceland, a sharp increase in *E. excavatum* 400 years ago was interpreted as severe condition in the fjord, representing the local marine signature of the LIA (Andrews et al., 2001).

Proxy-based temperature reconstruction from Haukadalsvatn, northwest Iceland, for the past 2000 years, characterized medieval times between ca. 900 and 1200 AD as a relatively warm period with higher productivity than before or after. However, cold spells were identified within that period in contrast to a stable warm period (Fig. 6-5) (Geirsdóttir et al., 2009). The first suggestion of LIA cooling occurred between 1250 and 1300 AD with a broad peak in TOC (Fig. 6-5). Geirsdóttir et al. (2009) interpreted peaks in TOC as an increased flux of carbon to the lake from eolian-derived soil erosion following periods of cold summers accompanied by dry, windy winters. The second interval of LIA cooling in Haukadalsvatn was between 1450 and 1500 AD, which lines up with a drop in the estimated bottom water temperature in Arnarfjörður (Fig. 6-5). Combined multi-proxy records from Haukadalsvatn and Hvítárvatn, are presented in figure 6-5. The DACP-MWP boundaries are not as evident from the lake records like in Arnarfjörður but the onset of colder conditions begins at similar times, around 1200 AD (Fig. 6-5). There are two temperatures drops from the combined records during the LIA which line up with two of the most severe temperature drops in Arnarfjörður. Vatnsdalsvatn, in northwest Iceland, lies in close proximity to the eastern part of Arnarfjörður. Nearly a 1000-year, decadal-scale record of the past environmental changes from that area detected higher erosion rates during the LIA (Doner, 2003). At Vatnsdalsvatn, the LIA is differentiated from the MWP (around 1350 AD) by slight increases in coarse magnetic grain size, magnetite concentration, TC, and terrestrial-carbon representation. Langdon et al. (2010) reconstructed summer temperature, from a lake in NW Iceland, reaching back to 1650 AD. The reconstruction is based on chironomid assemblages with a transfer function approach. The record was also compared against instrumental temperature measurements from Stykkishólmur in western Iceland. The reconstruction showed two clear phases of relatively cooler temperatures from1683 to 1710 AD, and 1765 to 1780 AD. Those two cold spells coincide with the coldest time period reported from Arnarfjörður.

6.4.2 North Iceland

A number of high-resolution studies have been made on core MD99-2275 (Eiríksson et al., 2006; Knudsen et al., 2012; Massé et al., 2008; Sicre et al., 2008), which is located on the shelf northeast of Iceland. One of these studies used IP25 biomarker produced by sea ice loving algae to reconstruct sea ice over the last millennium (Fig. 6-5) (Massé et al., 2008). The sea ice proxy shows no sea ice until ca. 1300 AD (MWP-LIA) when there is a small rise which lines up with a decrease in temperature in Arnarfjörður (Fig. 6-5). There is a second increase in IP25 and decrease in Arnarfjörður bottom water temperature around

1500 AD. The biggest IP25 peak is around 1600-1800 AD, which coincides with the coldest time in Arnarfjörður for the past 2000 years.

Sicre et al., (2008) reconstructed the sea surface temperatures (SSTs) for this same core (MD99-2275). The SSTs was warmer between 1000 and 1350 AD (Fig. 6-4), which was suggested to represent enhanced heat transport across the Denmark Strait by the NIIC. Sicre et al., (2008) concluded that reduced NIIC flow through the Denmark Strait during the LIA was likely resulting from higher freshwater and sea ice export from the Arctic. The SST data do not indicate clear evidence for colder conditions before the MWP like seen in the proxies from Arnarfjörður but the transition from the MWP to the LIA are clear around 1300 AD. Temperature and salinity reconstructions for the past 1000-year are also available from that same core (Knudsen, 2012). That reconstruction was based on transfer functions and oxygen isotopes for both planktic and benthic foraminifera. The MWP-LIA boundaries were defined by a general increase of Arctic Water indicator species at the transition. The earliest temperature change was seen in the bottom and subsurface waters, where a cooling was reconstructed as early as 1150–1200 AD. That is relatively early compared to the sea-surface changes and IP25 index from the same core (Massé et al., 2008; Sicré et al., 2008) but agrees with the BWT changes in Arnarfjörður. Knudsen et al. (2012) concluded that changes in the deeper water masses preceded long-term sea-surface and atmospheric changes at the MWP-LIA transition, and that short-term variability may have been influenced by the local wind circulation. Study, also from the North Icelandic shelf, with a shell-based chronology shows a falling trend in the shell growth, related to more colder climate, around ca. 1246 AD and lowered throughout the 17th century (Butler et al., 2013).
Reconstruction based on chironomid assemblages during the past 2000 years in Stóra Viðarvatn, northeast Iceland, showed that cold indicator species were more abundant in the second millennium than the first, particularly after 1200 AD (Axford et al., 2009). Cold periods were also characterized by intensified soil erosion and decreased lake productivity (Axford et al., 2009).

6.4.3 North Atlantic region

Eiríksson et al. (2006) studied palaeoceanographic variability, for the past 2000 years, along the eastern part of the North Atlantic. Four study sites were chosen, from North of Iceland all the way to the Iberian margin off Portugal. The DACP cooling period was not as evident in all of the records but they all showed an interval from 1300-1900 AD where the temperatures reached the lowest within the past two millennia.
Reconstruction of sea surface temperature, for the last 2000 years, from sediment cores north of Iceland and the subpolar North Atlantic where presented in Sicre et al. (2011). The two SST paleorecords were also compare to simulations. Comparison between the two sides showed that consistent multidecadal to centennial time-scale coolings occurred throughout the past millennium suggesting a strong connection between the two, related to regional hydrography and the NAC. The reconstruction found cooling of 1 to 2°C between about 1150 and 1300 AD. The model-data comparison suggested that this sequence of closely spaced volcanic eruptions could be responsible for the cold spell that interrupted the warm MCA conditons.

Hald et al. (2011) described changes in the Malangen fjord in Norway for the past 2000 years. In those records the DACP is reflected by a temperature minimum around 400 AD and 600–800 AD. In Arnarfjörður the lowest bottom water temperature for this period is at

ca. 450 AD and ca. 750 AD. In Malagen fjord the cooling characterizing the LIA starts around 1250 AD (Hald et al., 2011). High-resolution reconstruction from four marine cores from the eastern Norwegian Sea and adjacent Norwegian fjords, reflect temperature variability in the Atlantic Water, showed two periods from 1225–1450 AD and 1650–1905 AD when temperatures were 1.3 – 1.6°C lower than present (Klitgaard-Kristensen et al., 2004). They suggested that the cooling starting around 1300 AD was associated with a reduction in the strength of the thermohaline circulation.

6.5 Forcings

Variability in natural forcing causes changes in the climate. Those forcing can for example, be orbital variations, solar activity variations and large volcanic eruptions (Wanner et al., 2008). During the Holocene the long-term cooling of northern high-latitude regions has been linked to orbital forcing and its effects on insolation. That, however, cannot explain the multi-century climate variations of the past 2000 years. Other forcings, such as solar activity minima and volcanic eruptions, coinciding with the orbital forcing, are also believed to play a role (Wanner et al., 2008).

Changes in climate variability over the North Atlantic region have been explained for example with fluctuations of Atlantic Water in the northern North Atlantic (Hald et al., 2011), shutdown of deep water convection, sustained by sea ice formation , in the Nordic Seas in response to negative solar insolation anomalies (Berner et al., 2011), repeated explosive volcanism together with low summer insolation across the Northern Hemisphere (Miller et al, 2012), changes in solar activity (Jiang et al., 2015) and shifts in the NAO from positive mode to negative (Mann et al., 2009; Trouet et al., 2009).

An important amplifier of abrupt cooling and a mechanism to explain persistent cold summers is the expansion of Arctic Ocean sea ice and its export into the North Atlantic subpolar gyre. Miller et al. (2012) suggested that repeated explosive volcanism alongside low summer insolation across the Northern Hemisphere acted as a climate trigger resulting in increase in sea ice expansion. A sea ice/ocean feedback then maintained suppressed summer air temperature, long after the volcanic aerosols were removed from the atmosphere (Miller et al., 2012). Changes in the foraminifera fauna in Arnarfjörður show a clear sign of changes in the oceanic currents around Iceland, with intervals more influenced from the warmer Irminger current to times with more influence from colder currents. Changes in the NAO also seem to play a role in the environment in Arnarfjörður, with warmer and wetter conditions during the MWP compared to the LIA.

The timing and influence of volcanic eruptions for the past 2500 years were discussed in Sigl et al. (2015). In volcanic eruptions sulfate aerosol can be injected into the stratosphere shielding the Earth's surface from incoming solar radiations. Volcanic forcing is therefore one of the primary drivers of natural climate variability. Another forcing thought to be astrong driver of natural climate variability is the solar irradiation. Total solar irradiance reconstruction for the past 1200 years reveal five distinct grand solar minima during that time period (Steinhilber and Beer, 2011).

The BWT_{TF} from Arnarfjörður as well as combined proxies from Haukadalsvatn and Hvítárvatn and sea ice index from the North Iceland Shelf are compared with the global volcanic forcing and total solar irradiance for the past 2000 years in figure 6-6.

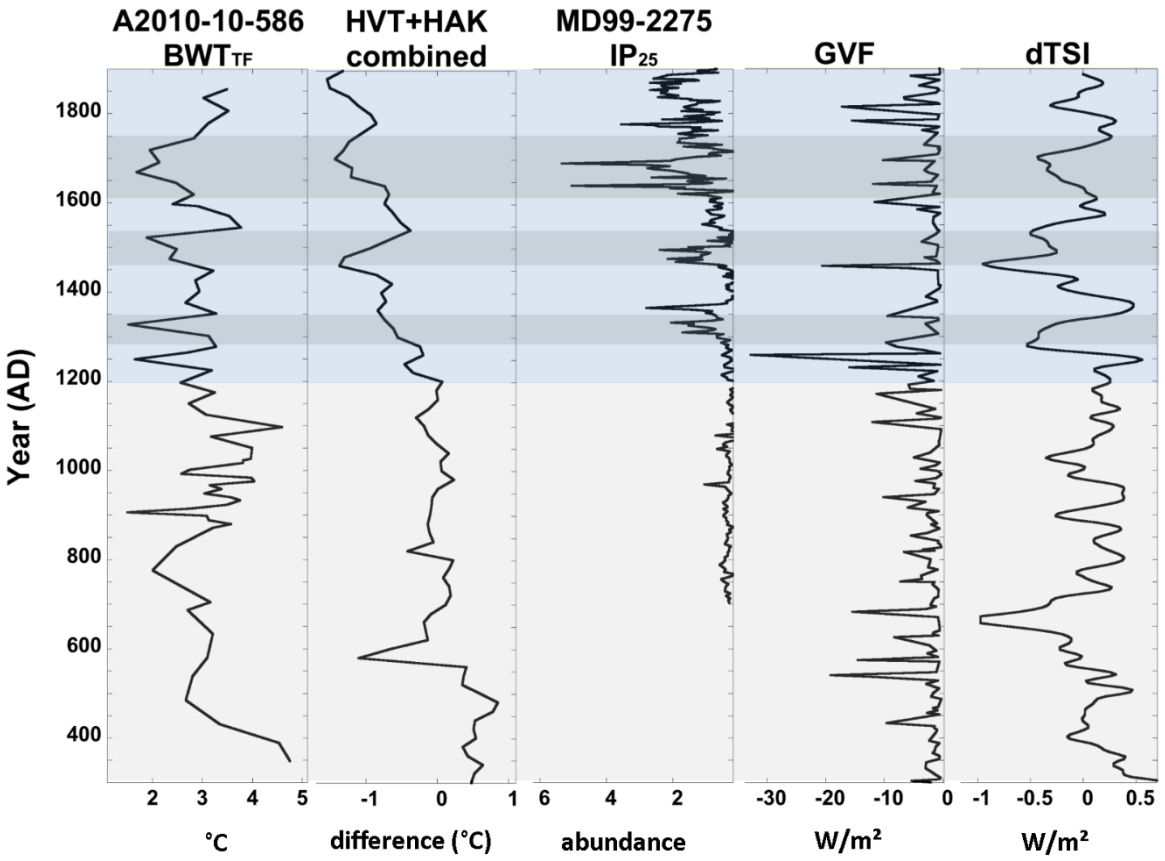

Figure 6-6: BWT_{TF} from Arnarfjörður, combined proxies from Hvítárvatn and Haukadalsvatn (Geirsdóttir et al., 2013), and SSTs from North of Iceland compared with Global Volcanic Forcing (GVF) (Sigl et al., 2015) and Total solarr irradiance (dTSI) (Steinhilber et al., 2009) (note that the sea ice index and GVF has been inverted so that it trends in the same direction as the other records).

The first drop in the BWT_{TF} in Arnarfjörður during the LIA coincides with a large volcanic signal around 1250 AD (Fig. 6-6). Between ca. 1450 – 1550 AD the BWT_{TF} from Arnarfjörður drops with increasing sea ice north of Iceland as well as a drop in temperature from the lake records. These cold spells line up with a large volcanic eruption (1458 AD) and decrease in the solar irradiance, known as the Spörer minima (1460-1550 AD). The coldest time period in Arnarfjörður is around 1650-1750 AD, during the time as the Maunder minima occurred (1645-1715 AD) and several large volcanic eruptions (Fig.6-6).

7 Summary and Conclusions

The proxy records from Arnarfjörður show several environmental changes occurring over the past 2000 years. *C. lobatulus* is the most dominant specie at the bottom part of the core but the arctic species *C. reniforme* and *E. excavatum* increase upwards. The core was divided into three time periods by applying Cluster Anlayses on the foraminiferal assemblages. The bottom part of the core (350 – 800 AD) shows a cooling but fairly stable condition (DACP). Between 800 – 1200 AD (MWP) the bottom water temperature increases and many of the Arctic species diminish. The MWP was wetter and warmer, under the influence of positive NAO. Coarser grained material was carried out to the fjord, possibly due to more precipitations, higher discharge from land to sea and stronger currents in the fjord eroding the coastline of Arnarfjörður. The MWP-LIA transition occurred around 1200 AD with a significant change in the faunal assemblage when arctic species increases and colder conditions start in the fjord. The proxies in the core from Arnarfjörður suggest that the LIA was very unstable and shifted from colder to less colder times. From ca. 1200-1400 AD the climate is cooling but after 1400 AD the conditions start to get harsher and there is a clear change in the faunal assemblage with *C. reniforme* and *E. excavatum* becoming the dominant species. The coldest time period in Arnarfjörður is around 1650-1750 AD (note: the core is missing the upper most 150yr) when there is a clear drop in BWT, TC and carbonate and increase in density, MS and IRD.

The climate and environmental variability in Arnarfjörður follow a similar trend as other paleoclimate records from Iceland. Changes in the ocean currents are clear from the foraminiferal assemblages. The coldest time periods in Arnarfjörður correlate well with known solar minima and increased volcanic activity and it is also evident that the MWP was much warmer and wetter than the LIA due to changes in the North Atlantic Oscillation. There are, however, some changes in the fjord that could be considered local variability, like the decrease in the wt% carbonate during the MWP. Studies from around Iceland usually show minimum in carbonate during the LIA, but due to freshwater effect in the fjord the carbonate values show lower values during the MWP. The other proxy records from the core correlate well with known records from land, however, the timing of those changes often vary regionally.

7.1 Further research

Continuation of this project would emphasize on couple of things:

1. Improve the age-model, possibly by searching for more crypto-tephra. Further studies of the local reservoir correction age (ΔR).

2. Extend the record closer to modern days (with a box core). This could help with interpretation of the data, and give the possibility of comparing with instrumental records. The time period between 1800 and 1900 AD is normally considered among the harshest in Iceland weather-wise, but this time period is mostly lost from the Arnarfjörður core.

3. Improve the proxy resolution based on sedimentation rate and age model. For the LIA the resolution for the foraminiferal counts is about 25 years. Changes in the mixing of the fjord water can result in anoxic conditions. Investigations of living benthic foraminifera in the surface sediments in Drammensfjord, southern Norway, from 1984-1989 showed that it took little over one year after reoxigenation, after more than five years of anoxic conditions, for the foraminfera to re-colonize the area (Alve, 1995). Higher resolution would improve the record and possibly prevent missing periods of potentially extreme conditions.

References

Alley, R. Agustdottir, A., and Fawcett, P. (1999). Ice-core evidence of late-Holocene reduction in North Atlantic ocean heat transport. In: Clark, P.U., Webb, R.S. and Keigwin, L.D. (editors) *Mechanisms of global climate change at millennial time scale,* 301-312.

Altenbach, A.V., Heeger, T. Linke, P., Spindler, M and Thies, A. (1993). Miliolinella subrotunda (Montagu), a miliolid foraminifer building large detritic tubes for a temporary epibenthic lifestyle. Marine Micropaleontology, 20, 293-301.

Alve, E. (1990). Variations in estuarine foraminiferal biofacies with diminishing oxygen conditions in Drammensfjord, SE Norway. Paleoecology, Biostratigraphy, Paleoceanography and Taxanomy of Agglutinated Foraminifera, 661-694. C. Hemleben et al. (eds). Kluwer Academic Publishers. Printed in Netherlands.

Alve, E. (1995). Benthic foraminiferal distribution and recolonization of formerly anoxic environment in Drammensfjord, Southern Norway. *Marine Micropaleontology, 25*, 169-186.

Andrews, J.T., Caseldine, C., Weiner, N.J. and Hatton, J. (2001). Late Holocene (ca. 4 ka) marine and terrestrial environmental change in Reykjarfjörður, north Iceland: climate and/or settlement? *Journal of Quaternary Science, 16* (2), 133-143.

Andrews, J.T. and Principato, S.M. (2002). Grain-size characteristics and provenance of ice-proximal glacial marine sediments. In: Dowdeswell, J.A. O'Cofaigh, C. (eds.). *Glacier-influenced Sedimentation at high-latitude*. Continental Margins, Geological Society of London, 305-324.

Andrews, J.T., Eberl, D.D. and Kristjansdottir, G.B. (2006). An exploratory method to detect tephras from quantitative XRD scans: ezamples from Icealnd and east Greenland marine sediments. *The Holocene, 16*(8), 1035-1042.

Andrews, J.T., Belt, S.T., Olafsdottir, S., Massé, G. and Vare, L.L. (2009). Sea ice and marine climate variability for NW Iceland/Denmark Strait over the last 2000 cal yr BP. *The Holocene, 19(*5), 775-784.

Andrews, J.T. and Jennings, A.E. (2014). Multidecadal to millennial marine climate oscillations across the Denmark Strait (~66°N) over the last 2000 cal yr BP. *Climate of the past, 10*, 325-343.

Axford, Y., Geirsdottir, Á., Miller, G.H. and Langdon, P.G. (2009). Climate of the Little Ice Age and the past 2000 years in northeast Iceland inferred from chironomids and other lake sediments. *J. Paleolimnol, 41*, 7-24.

Berner, K.S., Koc, N., Godtliebsen, F. and Divine, D. (2011). Holocene climate variabilitiy of the Norwegian Atlantic Current during high and low solar insolation forcing. *Paleoceanography, 26*(2).

Bradley, R.S. (1985). *Quaternary paleoclimatology: methods of paleoclimatic reconstruction*. Chapman and Hall, London.

Butler, P.G., et al. (2013). Variability of marine climate on the North Icelandic Shelf in a 1357-year proxy archive based on growth increments in the bivalve *Arctica islandica. Palaeogeography, Palaeoclimatolgoy, Palaeoecology, 373*, 141-151.

Cage, A.G., Heinemeier, J. and William, A. (2006). Marine rediocarbon reservoir ages in Scottish coastal and fjordic waters. *Radiocarbon, 48*(1), 31-43.

Doner, L. (2003). Late-Holocene paleoenvironments of northwest Iceland from lake sediments. *Palaeogeography, Palaeoclimatology, Palaeoecology, 193*, 535-560.

Einarsson, M.A. (1976). *Climate of Iceland*, In H. Van Loon (ed.) World survey of climatology. Vol. 45. Elsevier, Amsterdam, 673-697.

Eiríksson, J., Bartels-Jónsdóttir, H.B., Cage, A.G., Guðmundsdóttir, E.R., Klitgaard-Kristiansen, D., Marret, F., ... Sejrup, H.P. (2006). Variability of the North Atlantic current during the last 2000 years based on shelf bottom water and sea surface temperatures along an open ocean/shallow marine transect in western Europe. *The Holocene, 16*(7), 1017-1029.

Feyling-Hansen, R.W. (1972). The foraminifer Elphidium excavatum (Terquem) and its variant forms. *Micropaleontology, 18*(3), 337-354.

Geirsdóttir, Á., Miller, G.H., Thordarson, Th. and Ólafsdóttir, K.B. (2009). A 2000 year record of climatic variations reconstructed from Haukadalsvatn, West Iceland. *J Paleolimnol, 41*, 95-115.

Geirsdóttir, Á., Miller, G.H., Larsen, D.J. and Ólafsdóttir, S. (2013). Abrupt Holocene climate transition in the northern North Atlantic region recorded by synchronized lacustrine records in Iceland. *Quaternary Science review, 70*, 48-62.

Gooday, A.J. and Alve, E. (2001). Morphological and ecological parallels between sublittoral and abyssal foraminiferal species in the NE Atlantic: a comparison of *Stainforthia fusiformis* and *Stainforthia* sp. *Progress in Oceanography, 50*, 261-283.

Grobe, H. (1987). A simple method for the determination of ice-rafted debris in sediment cores. *Polarforschung, 57*(3), 123-126.

Guðmundsdóttir, E.R., Larsen, G., Eiríksson, J. (2012). Tephra stratigraphy on the North Icelandic shelf: extending tephrochronology into marine sediments off North Iceland. *Boreas*. DOI 10.1111/j.1502-3885.2012.00258.

Gunnarsdóttir, H. (2014). *Aukning framleiðslu Arnarlax á laxi í sjókvíum í Arnarfirði um 7.000 tonn/ári*. Mat á umhverfisáhrifum. Tillaga að matsáætlun, Verkís.

Hald, M., Steinsund, P.I., Dokken, T., Korsun, S., Polyak, L. and Aspeli, R. (1994). Recent and late Quaternary distribution of *Elphidium excavatum* f. *clavatum* in Arctic Seas. *Cushman Foundation Special Publication, 32*, 141-153.

Hald, M. and Steinsund, P.I. (1996). Benthic foraminifera and carbonate dissolution in the surface sediments of the Barents and Kara Sea. In: Stein, R., Ivanov, G.I., Levitan, M.A. and Fahl, K.

(publisher), *Surface sediments compostion and sedimentary processes in the central Arctic Ocean and along the Eurasian Continental margin*, Ber. Polarforsch, 295-307.

Hald, M. and Korsun, S. (1997). Distribution of modern benthic foraminifera from fjords of Svalbard, European Arctic. *Jornal of Foraminiferal Research, 27*(2), 101-122.

Hald, M., Kolstad, V., Polyak, Leonid, Forman, S.L., Herlihy, F.A., Ivanov, G. and Nescheretov, A. (1999). Late-glacial and Holocene paleoceanography and sedimentary environments in the St. Anna Trough, Eurasian Arctic Ocean margin. *Palaeogeography, palaeoclimatology, palaeoecology, 146*, 229-249.

Hald, M., Salomonsen, G.R., Husum, K. and Wilson, L.J. (2011). A 2000 year record of Atlantci water temperature variability from the Malangen fjord, northeastern North Atlantic. *The Holocene, 21*(7), 1049-1059.

Heier-Nielsen, S., Heinemeier, J., Nielsen, H.L. and Rud, N. (1995). Recent reservoir ages for danish fjords and marine waters. *Radiocarbon, 37*(3), 875-882.

Howe, J.A., Austin, W.E.N., Forwick, M., Paetzel, M. (eds). (2010). *Fjord systems and archives.* Geological Society, London, Sepcial Publications, 344, 5-15.

Hurrell, J.W. (1995). Decadal Trends in the North Atlantic Oscillation: Regional Temperatures and Precipitation. *Science, 260*(5224), 676-679.

Hurrell, J.W. (1996). Influence of variations in extratropical wintertime teleconnections on Northern Hemisphere temperature. *Geophysical research letters, 23*(6), 665-668.

Hurrell, J.W., Kushnir, Y., Ottersen, G. and Visbeck, M. (2003). An overview of the North Atlantic Oscillation: Climatic significance and environmental impact. *Geophysical monograph, 134*, 1-35.

Inall, M.E. and Gillibrand, P.A. (2010). The physics of mid-latitude fjords: a review. From Howe, J.A., Austin, W.E.N., Forwick, M. and Paetzei, M. (eds) *Fjord systems and archives*. Geological society, London, special publication, 344, 17-33.

Jennings, A.E. and Weiner, N.J. (1996). Environmental change in eastern Greenland during the last 1300 years: evidence from foraminifera and lithofacies in Nansen fjord, 68°N. *The Holocene, 6*(2), 179-191.

Jennings, A.E., Weiner, N.J., Harðardóttir, G. and Andrews, J.T. (2004). Modern foraminiferal faunas of the SW to N Iceland shelf: oceanographic and environmental controls. *Journal of foraminiferal research, 34*, 180-207.

Juggings, S. (2010). C2 Version 1.7.2 User Guide. *Software for ecological and paleoecological data analysis and visualization*, Newcastle University, Newcastel upon Tyne UK.

Klitgaard-Kristensen, D. And Sejrup, H.P. (1996). Modern benthic foraminiferal biofacies across the northern North Sea. *Sarsia, 81*, 97-106.

Klitgaard-Kristensen, D., Sejrup, H.P., Hafliðason, H. and Berstad, I.M. (2007). Eight-hundred-year temperature variability from the Norwegian continental margin and the North Atlantic thermohaline circulation. *Paleoceanography, 19*, doi:10.1029/2003PA000960.

Knudsen, K.L. and Seidenkrantz, M.-S. (1994). *Stainforthia feylingi* new species from arctic to subarctic environments, previously recorded as *Stainforthia schreibersiana* (CZJZEK). *Chusman foundation special publication, 32,* 5-13.

Knudsen, K.L. et al. (2012). Oceaonographic changes through the last millennium off North Iceland: Temperature and salinity reconstruction based on foraminifera and stable isotopes. *Marine Micropaleontology, 84-85,* 54-73.

Korsun, S.A., Pogodina, I.A., Forman, S.L. and Lubinski, D.J. (1995). Recent foraminifera in glaciomarine sediments from three arctic fjords of Novaja and Svalbard. *Polar research, 14(1),* 15-31.

Korsun, S. and Hald, M. (1998). Modern benthic foraminifera off Novaya Zemlya tidewater glaciers, Russian Arctic. *Arctic and Alpine Research, 30*(1), 61-77.

Korsun, S. and Hald, M. (2000). Seasonal dynamics of benthic foraminifera in a glacially fed fjord of Svalbard, European Arctic. *Journal of foraminiferal research, 30(4),* 251-271.

Kristensen, P. et al. (2000). Last Interglacial stratigraphy at Ristinge Klint, South Denmark. *Boreas, 29*, 103-116

Kristjánsdóttir, G.B., Stoner, J.S., Jennings, A.E., Andrews, J.T., Grönvold, K. (2007). Geochemistry of Holocene cryptotephras from the North Iceland Shelf (MD99-2269): intercalibration with radiocarbon and paleomagnetic chronostratigraphies. *The Holocene 17*(2), 155-176.

Kristjánsson, L. (2009). A new study of paleomagnetic directions in the Miocene lava pile between Arnarfjörður and Breiðafjörður in the Vestfirðir peninsula, Northwest Iceland. *Jökull, 59*, 33–50.

Larsen, G., Eiríksson, J., Knudsen, K.L. and Heinemeier, J. (2002). Correlation of late Holocene terrestrial and marine tephra markers, north Iceland: implications for reservoir age changes. *Polar Research, 21(2),* 283-290.

Logemann, K., Ólafsson, J., Snorrason, Á., Valdimarsson, H. and Marteinsdóttir, G. (2013). The circulation of Icelandic waters-a modellingy study. *Ocean Science, 9*, 931-955.

Lougheed, B.C., Filipsson, H.L. and Snowball. I. (2013). Large spatial variations in coastal 14C reservoir age-a case study from the Baltic Sea. *Clim. Past, 9*, 1015-1028.

Mann, M. E. et al. (2009). Global signatures and dynamical origins of the little ice age and medieval climate anamaly. *Science, 326*. 1256-1260.

Massé, G. et al. (2008). Abrupt climate changes for Iceland during the last millennium: Evidence from high resolution sea ice reconstructions. *Earth and Planetary Science Letters, 269*, 565-569.

Miller, G.H. et al. (2012). Abrupt onset of the little Ice Age triggered by volcanism and sustained by sea-ice/ocean feedbacks. *Geophysical research letters, 39*.

Murray, J.W. (1991). *Ecology and palaeoecology of benthic foraminifera*. Longman Scientific and Technical, Essex.

Murray, J.W. (2001). The niche of benthic foraminifera, critical thresholds and proxies. *Marine Micropaleontology 41*, 1-7.

Nordberg, K., Gustafsson, M. and Krantz, A.-L. (1999). Decreasing oxygen concentration in the Gullmar fjord, Sweden, as confirmed by benthic foraminifera, and the possible association with NAO. *Journal of Marine Systems, 23*, 303-316.

Olsen, J., Rasmussen, P. and Heinemeier, J. (2009). Holocene temporal and spatial variation in the radiocarbon reservoir age of three Danish fjords. *Boreas, 38*(3), 458-470.

Ólafsdóttir, S. (2004). Currents and climate on the northwest shelf of Iceland during the deglaciation: high-resolution foraminiferal research. Unpublished MSc thesis, University of Iceland.

Ólafsdóttir, S., Jennings, A.E., Geirsdóttir, Á., Andrews, J. and Miller, G.H. (2010). Holocene variability of the North Atlantic Irminger current on the south- and northwest shelf of Iceland. *Marine Micropaleontolgoy, 77*, 101-118.

Polyak, L., Korsun, S., Febo, L.A., Stanovoy, V. and Khusid, T. (2002). Benthic foraminiferal assemblages from the southern Kara Sea a river-influenced arctic marine environment. *Journal of foraminiferal research, 32(3),* 252-273.

Polyak, L., Alley, R.B., Andrews, J.T., Brigham-Grette, J., Cronin, T.M., Darby, D.A. et. al. (2010). History of sea ice in the Arctic. *Quaternary Science Reviews, 29*, 1757-1778.

Quillmann, U., Jennings, A. and Andrews, J. (2010). Reconstructing Holocene palaeoclimate and palaeoceanography in Ísafjarðardjúp, northwest Iceland, from two fjord records overprinted by relative sea-level and local hydrographic changes. *Journal of Quaternary Science, 25*(7), 1144-1159.

Reimer, P.J., Bard, E., Bayliss, A., Beck, J.W., Blackwell, P.G., Ramsey, C.B.,.....,van der Plicht, J. (2013). IntCal13 and MARINE13 radiocarbon age calibration curves 0-50000 years calBP. *Radiocarbon, 55*(4), 1869-1887.

Rytter, F., Knudsen, K.L., Seidenkrantz, M.-S. and Eiríksson, J. (2002). Modern distribution of benthic foraminifera on the north Icelandic shelf and slope. *Journal of foraminiferal research, 32(3),* 217-244.

Sejrup, H.P., Birks, H.J.B., Klitgaard-Kristensen, D. And Madsen, H. (2004). Benthonic foraminiferal distributions and quantitative transfer functions for the northwest European continental margin. *Marine Micropaleontology, 53*, 197-226.

Sicre, M.-A., et al, (2008). Decadal variability of sea surface temperature off North Iceland over the last 2000 yrs. *Earth and Planetary Science Letters, 268*, 137-142.

Sicre, M.-A., Hall, I.R., Mignot, J., Khodri, M., Ezat, U., Truong, M.-X., Eiríksson, J., et al. (2011). Sea surface temperature variability in the subpolar Atlantic over the last millennia. *Paleoceanography, 26*, PA4218, doi:10.1029/2011PA002169

Sigl, M., Winstrup, M., McConnell, J.R., Welten, K.C., Plunkett, G., Ludlow, F. et al. (2015). *Timing and climate forcing of volcanic eruptions for the past 2500 years*. Nature. doi: 10.1038/nature14565.

Sigurðsson, O. (2004). Gláma, að vera eða vera ekki-jökull. *Náttúrufræðingurinn, 72(1-2),* 47-61.

Steele, J.H., Thorpe, S.A., Turekian, K.K. (2009). *Elements of physical oceanography*. Science, 520.

Stefánsson, U. (1999). *Hafið*. Reykjavík. Háskólaútgáfa.

Steinhilber, F., Beer, J., Fröhlich, C. (2009). Total solar irradiance during the Holocene. Geophys. Res. Lett., 36, L19704, doi: 10.1029/2009GL040142.

Steinhilber, F. and Beer, J. (2011). Solar activity – the past 1200 years. *Pages news, 19(*1), 5-6.

Stuiver, M. and Reimer, P.J. (1993). Extended ^{14}C base and revised Calib 3.0 ^{14}C age calibration program. *Radiocarbon, 35(1)*, 215-230.

Thompson, D.W.J. and Wallace, J.M. (1998). The Arctic Oscillation signature in the wintertime geopotential height and temperature fields. *Geophysical research letters, 25*(9), 1297-1300.

Thors, K. (1974). "Sediments of the Vestfirdir shelf, NW-Iceland and geology of the Úlfarsfell area, SW-Iceland." Victoria University of Manchester.

Trouet, V., Esper, J., Graham, N.E., Baker, A., Scourse, J.D. and Frank, D.C. (2009). Persistent positive North Atlantic oscilliation mode dominated the Medieval climate anomaly. *Science, 324*, 78-80.

Valdimarsson, H., and Malmberg, S-A. (1999). Near-surface Circulation in Icelandic Waters derived from satellite tracked driftters. *Rit Fiskideildar, 16*, 23-39.

Wadhams, P. (2000). *Ice in the Ocean*. Gordon and Breach Science Publishers.

Wanner, H., Solomina, O., Grosjean, M., Ritz, S.P., and Jetel, M. (2011). Structure and origin of Holocene cold events. *Quaternary Science review, 30*, 3109-3123.

Hafrannsóknarstofnun Íslands. (2015). www.hafro.is (online) Available at http://www.hafro.is/index.php. (Last accessed 1. September 2015).

Hurell, J. and National Center for Atmospheric Research Staff (Eds). Last modified 07 Jul 2015. "The Climate Data Guide: Hurrell North Atlantic Oscillation (NAO) Index (station-based)." Retrieved from https://climatedataguide.ucar.edu/climate-data/hurrell-north-atlantic-oscillation-nao-index-station-based. –See more at: https://climatedataguide.ucar.edu/climate-data/hurrell-north-atlantic-oscillation-nao-index-station-based#sthash.NBEa36yX.dpuf.